Study of a Microcomposite Metal-Doped

Polyimide Adhesive

by

Laura Lynne Smith

Thesis submitted to the Faculty of the

Virginia Polytechnic Institute and State University

in partial fulfillment of the requirements for the degree of

Master of Science

in

Materials Engineering

APPROVED:

James P. Wightman, Chairman

John G. Dillard

Guy R. Wilson

June, 1989

Blacksburg, Virginia

Study of a Microcomposite Metal-Doped

Polyimide Adhesive

by

Laura Lynne Smith

James P. Wightman, Chairman

Materials Engineering

(ABSTRACT)

It is widely held in the field of adhesion science that the properties of the interfacial region, or interphase, between two bonded surfaces are of critical importance to the performance of an adhesive bond. This thesis describes a study in which a polyimide was modified by the addition of metal compounds in an effort to develop a graded interface between the adhesive and aluminum adherends. The results of mechanical adhesion testing and instrumental analysis of the failed surfaces indicated that the added compounds did in fact preferentially segregate toward the adherend surfaces, but that this segregation decreased the strength of bonds tested in peel. It was concluded that the collection of metal compounds at the metal surfaces did not occur in such a manner as to improve the integrity of adhesive bonds, but the possibility remains that an improved, graded interface might still be formed given a more appropriate adhesive/dopant system and improved specimen preparation and testing techniques.

Dedication

To my excellent husband, : a truly decent human being.

Acknowledgements

The work described in this thesis would not have been possible without the contributions of many people and organizations. The author gratefully acknowledges their efforts.

First, I would like to thank my advisor, Dr. J. P. Wightman, for his inspiration, patience, encouragement, and support and for providing opportunities to attend meetings and meet prominent researchers. I would also like to thank my other committee members, Dr. J. G. Dillard and Dr. G. R. Wilson, for serving on my committee and for their contributions to my research and overall experience.

I would like to thank the other main contributors to this joint project: Dr. L. T. Taylor and Dr. J. D. Rancourt for their earlier and ongoing research in the area and helpful discussions, and for his useful observations and invaluable lab work in preparing materials and specimens.

I would like to express my appreciation for the support and guidance of Dr. Karl Wefers and the Alcoa Technical Center, and for providing materials, funds, and helpful comments.

I am grateful for the support of the Adhesive and Sealant Council, which provided a graduate fellowship. I thank the Center for Adhesive and Sealant Science at Virginia Tech for providing the opportunity for the fellowships and for allowing students to establish good relationships in the field while in school.

I would like to thank the indispensible and long-suffering for his decency and competence in running samples, instructing students, and keeping the equipment functioning. I would like to thank and for good STEM work, and the innumerable other support personnel who keep everything running.

I would like to thank an assortment of other grad students, including , , , , , and , for answering stupid questions, passing on their tricks and expertise, and for gratuitous comments, criticism, advice, kibitzing, ideas, and friendship.

Finally, I would like to thank my family: my parents, my sisters and brother, and my in-laws, for their love and support; our cat, , for helping me with my thesis (sitting on books, papers, etc.); and my husband for his computer and his understanding and support throughout my graduate experience.

Table of Contents

I. Introduction **1**

II. Literature Review **6**

A. Fundamental Descriptions of Adhesion 6

1. Thermodynamic Work of Adhesion 6

2. Theories of Adhesion 9

B. Metal Modification of Polyimide Adhesives 10

1. Condensation Polyimides 10

a. Development 10

b. Properties and Applications 12

2. Metal Modification 13

a. Review 13

b. Studies of Polyimides Modified With Dissolved Metal Compounds 14

C. Adhesive Bonding of Aluminum 17

1. Aluminum Surfaces 17

2. Pretreatments for Adhesive Bonding 18

a. Degreasing 18

b. Simple Etches 19
c. FPL Etch 19
d. Conversion Coatings 21
e. Anodization 21
3. Environmental Effects on Bonds with Aluminum 22
D. Mechanical Adhesion Testing 22
1. Overview 22
2. The Floating Roller Peel Test 24
E. Surface Analysis 26
1. Electron Microscopy 26
2. X-ray Photoelectron Spectroscopy 30

III. Experimental Approach 34
A. Materials 34
1. Aluminum Adherends 34
2. Polyimide Adhesive System 35
B. Specimen Preparation 37
1. Surface Pretreatment 37
2. Peel Test Specimens 37
a. Application of Adhesive 37
b. Bonding Procedure 38
3. Surface Analysis Specimens 41
C. Peel Testing 41
1. Variation of Peel Rate 41
2. Elevated Temperature Testing 42
3. Variation of Dopant Concentration 42
4. Effects of Pre-cure Temperature and Surface Pretreatment 43
5. Environmental Exposure 43

D. Surface Analysis 44
1. SEM 44
2. XPS 44

IV. Results and Discussion **45**
A. Preliminary Experiments 45
1. SEM of Pretreated Foil Surfaces 45
2. Single Adhesive Layer Bonds 49
3. Variation of Pre-cure Temperature 50
4. Elevated Temperature Study 52
5. Variation of Dopant Concentration 52
6. Conclusions 55
B. Study of Doping, Pre-cure, and Surface Pretreatment 57
1. Peel Test Matrix 57
2. Results 59
a. Pre-cure Temperature 59
b. Surface Pretreatment 59
c. Dopant Concentration 61
3. Analysis of Failed Surfaces 62
a. SEM 62
b. XPS 65
C. Elevated Temperature Study 77
D. Environmental Exposure Study 77

V. Summary **80**
A. Conclusions 80
B. Recommendations for Further Study 81

VI. References 83

Vita 88

List of Illustrations

Figure 1. Illustration of a gradient of properties across a metal-adhesive interface. 4

Figure 2. Schematic illustration of the forces governing a contact angle [13]. 8

Figure 3. General scheme of conventional PI synthesis. 11

Figure 4. Isometric drawings of oxide structures on (a) FPL etched surface and (b) phosphoric acid anodized surface [51]. 20

Figure 5. Examples of peel test configurations: (a) 180° peel (b) 90° peel (c) drum peel (d) T-peel (e) floating roller peel [71]. 25

Figure 6. Schematic drawing of SEM instrument [77]. 28

Figure 7. Secondary electron detection system for (a) SEM and (b) STEM [78]. 29

Figure 8. Schematic diagram of XPS analysis [81]. 31

Figure 9. Polyimide system used in this study. 36

Figure 10. Illustrations of specimen preparation: (a) straightedge for drawing films (b) one batch ready for bonding (c) completed peel specimen. 39

Figure 11. Diagrams of bonding configurations: (a) Coupon layer + foil layer (b) coupon layer only (c) doped film on coupon (d) doped film on foil. 40

Figure 12. High-resolution SEM of acetone-wiped Al foil surface, 50,000X; white bar = 50 nm. 46

Figure 13. High-resolution SEM of NaOH-etched Al foil surface, 50,000X; white bar = 50 nm. 47

Figure 14. High-resolution SEM of FPL-etched Al foil surface, 50,000X; white bar = 50 nm. 48

Figure 15. Peel load vs. displacement plots for specimens tested at (a) 190°C and (b) 195°C. 54

Figure 16. Photograph of peel specimens, failure at (a) foil-adhesive interface (b) between adhesive layers (c) mixed; some at adhesive-coupon interface. 60

Figure 17. SEM images of failed peel surfaces, 2000X: undoped adhesive (a) foil side (b) adhesive side. 63

Figure 18. SEM images of failed peel surfaces, 2000X: BTDA/APB//$CoCl_2$ (a) foil side (b) adhesive side. 64

Figure 19. C 1s photopeaks obtained from (a) cured polyimide surface and (b) failed foil surface. 66

Figure 20. Al 2p photopeak obtained from failed foil surface, showing contribution from Al^0 as well as Al_2O_3. 67

Figure 21. Co 2p photopeaks obtained from (a) failed adhesive surface and (b) failed foil surface. 73

Figure 22. Suggested general scheme for bond structure and locus of failure. 76

Figure 23. Effect of hot water (70°C) exposure prior to peel testing. 78

List of Tables

Table 1. Results of variation of pre-cure temperature. 51

Table 2. Results of elevated temperature peel testing. 53

Table 3. Results of variation of dopant concentration. 56

Table 4. Peel strengths as a function of pre-cure, surface pretreatment, and dopant level; peel strength values in N/cm. 58

Table 5. Representative XPS atomic concentrations and binding energies for air-cured polyimide surfaces. 70

Table 6. Representative XPS atomic concentrations and binding energies for failed surfaces of peel specimens. 71

Table 7. Peel strengths and C.E.F.s for failed foil surfaces. 75

I. Introduction

The practice of using adhesives to join or bond materials has a long history and dates back thousands of years. The ancient Egyptians and Babylonians made use of bitumen, gum Arabic, animal glues, pastes, and other substances for a variety of bonding applications; the Egyptians, for example, were using adhesives to bond papyrus and veneer furniture at least as early as 1350 B.C. [1,2]. In fact, these ancient civilizations employed technology in adhesives which was subsequently lost and had to be rediscovered by medieval Europeans. Despite the age-old use of adhesives, however, adhesion as a science is of recent development and is only about 40 years old. The past three decades have seen a remarkable increase in the number of adhesive products developed, and it is estimated that between 1971 and 1986 the consumption of adhesives by volume in the U.S. and Europe increased approximately twice as fast as the respective gross national products [1]. The scope of adhesive bonding in general has also been widened. Research has resulted in adhesives capable of bonding many different materials in a wide variety of configurations and environmental conditions. Man's growing knowledge of surface science and polymeric materials, and the formulation of scientific theories and approaches with regard to adhesion, have made this significant technological development possible [1,3].

One of the underlying reasons for this growth in the use of adhesives has been the broadening of the field to include the bonding of materials not traditionally joined with adhesives, such as

metals. Conventional fastening techniques for metals, such as welding and riveting, are adequate for many applications, but have some crucial vulnerabilities under certain circumstances. For example, the so-called heat-affected zones surrounding welds are often weaker, more brittle, and are more susceptible to corrosion and stress-corrosion cracking than the parent metal. Also, the abrupt and intense heating cycle involved in the welding process often results in fine shrinkage cracks in the welds and surrounding material [4]. Riveted parts are not without their problems as well; aside from the fact that the use of mechanical fasteners adds weight to the final structure, the very presence of holes in the material for the rivets causes the concentration of stresses around the holes when the structure is loaded. In addition, both the riveted part and its fasteners are subject to a variety of failures which would not threaten the structure were it joined in some other way [5]. The use of suitable adhesives for joining metal avoids these characteristic problems, allows the distribution of loads over larger areas, saves weight, and permits the design of more efficient structures.

In order for organic adhesives to replace successfully other joining technologies for metals in many applications, the adhesives must be able to perform satisfactorily under the same conditions as other joining methods. Important restrictions on the applications of these materials still exist; for example, one of the most critical drawbacks of polymeric adhesives is their lack of stability at very high temperatures - 500°C and above. The class of polymeric materials known as polyimides (PIs) was originally developed in the early 1960s during the search for polymers with increased stability at elevated temperatures. The early PIs were insoluble and infusible once fully imidized and released large quantities of volatiles - chiefly H_2O - in the process of curing, making processing and practical use as adhesives difficult [3]. Since then, various approaches have been taken toward developing new polyimide systems for different adhesive roles; some of these are discussed in detail in the next chapter.

The goals of researchers and others who work to develop and improve adhesives are to devise adhesive systems which can maintain the integrity of bonded joints under the necessary loading and environmental conditions, which can be processed into easy-to-apply forms, and which do not require exceptionally time-consuming and expensive storage and preparation techniques for their use. These are tough requirements in many ways, but great strides in adhesion research have been made

in the past generation. An interdisciplinary, scientific basis for adhesion now exists and continues to grow, drawing from the expertise of workers in surface science, chemistry, polymer science and engineering, and materials science and mechanics. Working together and pooling their knowledge, specialists in these areas are addressing the limitations of polymeric adhesive systems seeking to overcome them.

The development and application of modern composite materials are fields which, like adhesion science, are interdisciplinary and are resulting in greater understanding of certain principles in the same areas of science mentioned above. The potential benefits to be obtained from combining the properties of substantially different materials have yet to be fully realized. Among the most important issues growing out of research in these areas is the characterization of the interactions between the materially different components of composite structures. It is now generally believed that the interface between these components plays a critical role in the bulk properties of the material or part; similarly, the interfacial region or interphase has been identified as being of critical importance to the behavior of adhesive bonds [6,7]. In light of these views, it is supposed that improvements in the material properties of the interphase region - specifically, its ability to transfer stress and to dissipate fracture energy - would improve the overall integrity of a bonded system. Consequently, the formation of a materially graded interface will result in greater mechanical strength and durability of an adhesive bond.

Taylor and co-workers have conducted extensive studies over the past ten years on the doping of polyimide and polysiloxane films with metal compounds [8-11]. It was found in many cases that metal salts added to the polymers converted to metallic or oxide form and segregated towards the surfaces of the films upon curing, sometimes forming layered or graded microstructures in the near-surface regions of the films. Polyimide properties altered by this method of metal modification include: a) improved elevated temperature adhesive properties in bonded metal joints [9], b) increased surface and volume electrical conductivity [10], c) increased modulus in flexible films [11], and d) improved high temperature tensile strength [12]. It is supposed that the peculiar segregation of metal in these polymers can result in a gradient of properties from the bulk polymer to the substrate, thereby producing a superior adhesive bond. This concept is illustrated schematically in

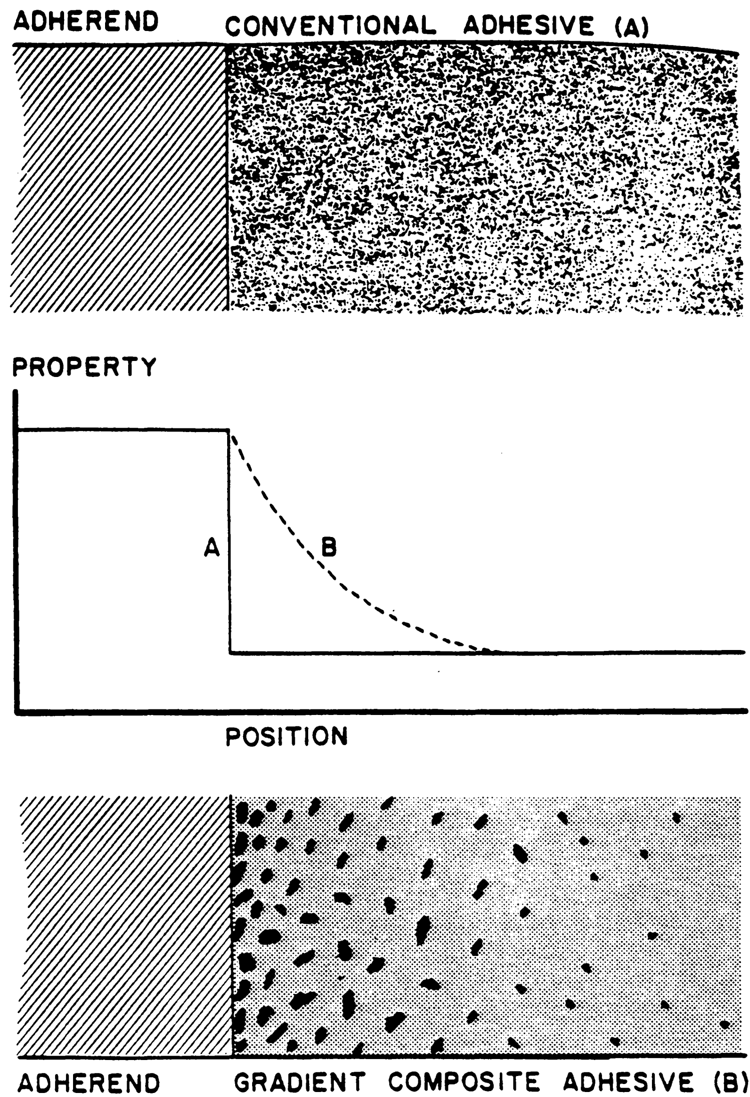

Figure 1. Illustration of a gradient of properties across a metal-adhesive interface.

Figure 1. Such modification may improve the performance of polyimides in their role as high-strength, high-temperature adhesives.

This thesis describes a study conducted to explore this graded-interface concept in connection with the adhesive bonding of aluminum. Prior to this study no systematic evaluation of metal-modified polyimides as adhesives had been conducted. A particular polyimide and metal compound system was chosen based on the results of Taylor's previous work, and specimens were produced using aluminum adherends and the polyimide systems as adhesives. Mechanical adhesion testing and various surface analytical techniques were performed in an effort to determine whether the previously described segregation phenomena occur *in situ* in an adhesive bond, and whether the resulting graded interface in fact improves the performance of the bond under various conditions. Interpretation of the results of this study should provide information on the possible strengthening of the interphase region between aluminum and microcomposite polyimides due to improved mechanical properties of the near-surface region of adhesive layers.

II. Literature Review

A. Fundamental Descriptions of Adhesion

1. Thermodynamic Work of Adhesion

Most adhesives, at some point in the formation of an adhesive bond, are in liquid form and are in contact with the solid adherend surfaces. Thermodynamic relationships describing liquid-solid interactions can be used in the study of adhesive bonding. When a liquid comes in contact with a solid surface, the question of whether the liquid spreads and wets the surface or "beads up" is determined by the surfaces' relative *surface free energy* γ, often referred to as surface tension in the case of liquids. The thermodynamic work of adhesion W_a - which can be described as the reversible energy input required to separate the surfaces of two different materials in intimate contact - can be expressed in terms of the free energy of the solid surface γ_{SV}, the free energy of the liquid surface γ_{LV} (both surfaces in equilibrium with the vapor), and the free energy of the solid-liquid interface γ_{SL}:

$$W_a = \gamma_{SV} + \gamma_{LV} - \gamma_{SL} \qquad \text{[II.1]}$$

The work of adhesion can also be expressed in terms of γ_{LV} and the contact angle θ, defined to be the angle between the flat solid surface and the tangent to a liquid droplet's surface at the point of contact as illustrated in Figure 2:

$$W_a = \gamma_{LV}(1 + \cos\theta) \qquad \text{[II.2]}$$

The spreading pressure π is assumed to be negligible in this equation.

Fowkes [14] proposed that the interaction between molecules across an interface could be subdivided into several components consisting of dispersion forces (d), dipole-dipole interactions (p), hydrogen bonding (h), induced dipole (i), and acid-base interactions (ab) so that

$$W_a = W_a^d + W_a^p + W_a^h + W_a^i + W_a^{ab} \qquad \text{[II.3]}$$

Similarly,

$$\gamma = \gamma^d + \gamma^p + \gamma^h + \gamma^i + \gamma^{ab} \qquad \text{[II.4]}$$

For interactions between two phases which involve only dispersion forces, the interfacial free energy γ_{SL} can be expressed as

$$\gamma_{SL} = \gamma_{SV} + \gamma_{LV} - 2(\gamma_S^d \gamma_L^d)^{1/2} \qquad \text{[II.5]}$$

Thus, when only dispersion forces are present, the work of adhesion depends only on the dispersion components of the surface free energies and can be written

$$W_a = 2(\gamma_S^d \gamma_L^d)^{1/2} \qquad \text{[II.6]}$$

The subjects of spreading, wetting, and interactions of surfaces are very interesting and quite extensive, and need not be detailed here. The fundamentals can be found in any good physical

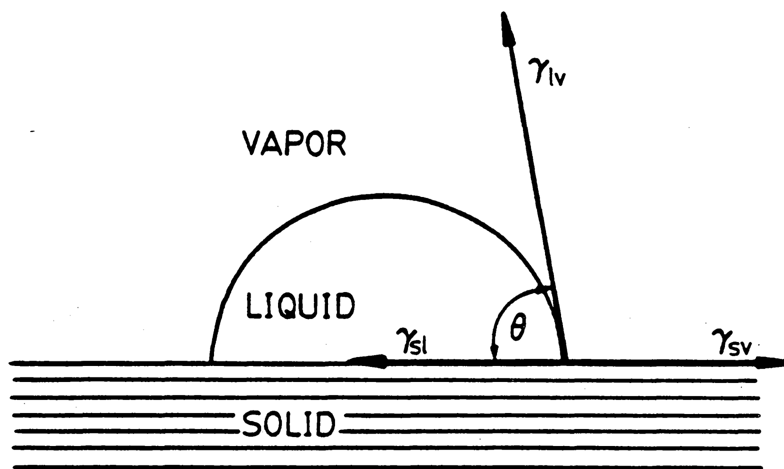

Figure 2. Schematic illustration of the forces governing a contact angle [13].

chemistry or surface chemistry text [15,16] and descriptions of these principles with respect to adhesion are offered in a number of review articles on the subject [17].

2. Theories of Adhesion

A number of theories or mechanisms for adhesion have been proposed over the years, and for a given bonding situation any one or combination of them may be appropriate to describe the dominant principles at work. To date, six mechanisms of adhesion have been proposed, according to Anderson [2]. *Mechanical interlocking*, also called *hooking*, of the adhesive and adherend is thought to occur when liquid adhesive flows into and fills microscopic cracks in the adherend, hardens, and afterward is not removable. This type of joining requires the liquid adhesive be sufficiently fluid, and the adherend sufficiently wet by the liquid, that it can easily penetrate even small cracks or pores in a short time. Such penetration has been demonstrated to occur, as in the work by Ko [8], for example. The *diffusion theory*, which is specifically concerned with polymer-polymer bonding, suggests that the polymeric molecules of adhesive and adherend diffuse into one another. This physical bond formed of entangled molecules is, in a sense, not unlike mechanical interlocking. The *electrostatic theory* concerns the attraction between adhesive and adherend as a result of charge developed from the transfer of electrons between the two surfaces. This mechanism is proposed not as a primary bonding cause but rather as a strengthening factor; for many adhesives, however, this electrostatic contribution is small or negligible. The *adsorption theory* is simply a statement that London dispersion forces, dipole-dipole interactions, and dipole-induced dipole attractions between the adhesive and adherend will contribute to adhesive bonding. These forces do, in fact, contribute significantly; alone they can adequately account for adhesive strengths in many bonds. Similar to the adsorption theory, the *chemical reaction* theory proposes that actual chemical bonds - ionic, covalent, or metallic - are formed across the adhesive-adherend interface from chemical reactions between the two surfaces. Yet another variation on this theme is the contribution of *acid-base interactions* to adhesive bonding, considering either the Brønsted or Lewis concepts of acids

and bases. This sort of attraction between adhesive and adherend surfaces is believed to contribute a significant part to bond strength in some systems, and is becoming an important concept to take into account when designing or engineering an adhesive system [2,18-20].

B. *Metal Modification of Polyimide Adhesives*

1. Condensation Polyimides

a. Development

After a need for structural adhesives with high elevated temperature stability was recognized in the late 1950s, a major effort was initiated to develop them. At about the same time, the development of organic polymers with high thermal stability was reported; however, these polymers were noted for their very poor processability. Research in the area began to be devoted to developing these thermally stable polymers into processible forms, and to evaluating these materials as adhesives and composite matrices [3].

Polyimides (PIs) were among the polymer systems initially investigated in this effort. Early examples of PI synthesis employed the method of Edwards [21] and Endrey [22], in which a soluble polyamic acid was formed from the stoichiometric condensation reaction of a diamine and a tetracarboxylic acid dianhydride as shown in Figure 3. This polyamic acid was then dehydrated - usually thermally - to effect ring closure and form the polyimide. The resulting early PIs were infusible and insoluble, and the evolution of volatile water during imidization often caused difficulties in processing as adhesives. In addition, the polyamic acid precursors tended to be susceptible to hydrolysis [23].

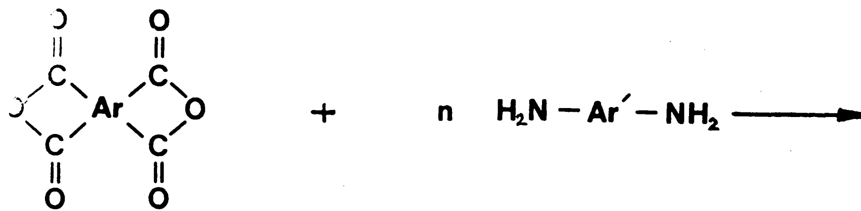

Ar and Ar′ = aromatic

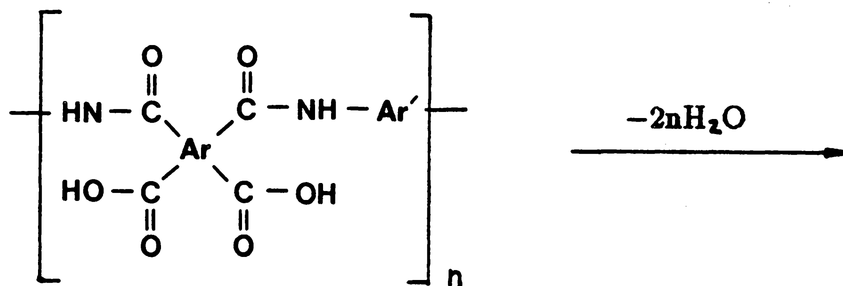

polyamic acid

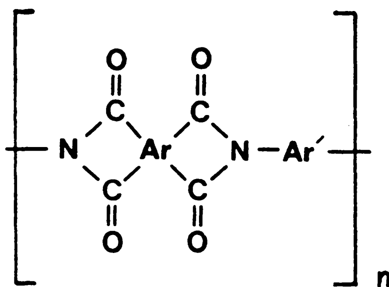

polyimide

Figure 3. General scheme of conventional PI synthesis.

Efforts have been made to process PIs as thermoplastics, above their glass transition temperatures (T_gs), in order to circumvent the problem with volatiles. Burgman and co-workers [24] were the first to succeed in this; related work by Progar and St. Clair [25] resulted in the development of LaRC-TPI as an adhesive with elevated temperature stability. Today the primary use of LaRC-TPI is in circuit boards designed for high temperature environments.

b. Properties and Applications

Polyimides derived from aromatic dianhydrides and aromatic diamines exhibit outstanding thermal stability. The range of T_g for PIs is broad - 50-400°C - and is strongly dependent on the molecular structure; stiffer and more branched backbone chains tend to raise the T_g, for example. Most polyimides are quite solvent-resistant, to polar and non-polar solvents alike, though the aromatic polyetherimides are susceptible to a range of solvents from chlorinated hydrocarbons to N,N-dimethyl formamide (DMF) and N,N-dimethyl acetamide (DMAc). Matching a solvent with a polyimide for a given application is difficult to do predictively, and for all practical purposes must be done empirically [26]. Mechanically, polyimides generally exhibit toughness, good impact strength, high flexural stiffness, and excellent tensile, compressive, and flexural strengths. Stiffness can be increased further by the addition of fillers such as glass, metal, carbon powder, or mineral matter. PIs tend to be rather brittle and exhibit only modest tensile enlongation, between 2 and 10% [27]. Electrically, PIs are good insulators while having relatively low dielectric constants.

This variety of properties makes polyimides well suited for many applications. Kapton® is an example of a polyimide which, as an adhesive tape and a polymer film, has become a well-known and valuable item in many workplaces because of its high thermal stability. The high stiffness and compressive strengths of polyimides have resulted in the wide use of PIs in load-bearing situations such as struts, chassis and brackets in automotive and aircraft structures. The ability of PIs to maintain dimensional stability under load makes them useful in high temperature bearings. In the electronics industry, polyimides are becoming widely used in many areas; they are

replacing glass and ceramics in insulators and switches, used for printed circuit board material, and are being used increasingly as spin-cast thin films for insulating and passivating layers in integrated circuits. Last but not least, polyimides are steadily finding increasing use as adhesives for high-temperature applications, and currently remain the front-runner materials in the area [28]. For many reasons, then, polyimides are high performance materials and are considered specialty plastics. As such, they are priced accordingly and are much more expensive than commodity items such as polyethylene or polystyrene. Because of their outstanding properties and yet-to-be-fully-realized potential, polyimides development remains an active area of research [26].

2. Metal Modification

a. Review

Modification of the physical and chemical properties of polyimides in general is a broad and expanding field of science, and the incorporation of metallic species into polymers is an active area of research within this field [29,30]. St. Clair and Taylor [30] have provided a good review of the latter subject, which they have divided into five general categories. One type of study involves polymers having covalently attached ionic groups which are neutralized by a metallic counterion [31]. Incorporation of the metal ion may occur after formation of the ionic polymer, or a metal salt monomer may be employed in effecting the polymerization. A second, and large, area of metal-polymer studies includes polymers having metal atoms organically bonded into the polymer back-bones; these may correctly be called organometallic polymers. A third group of metal-polymer systems may be represented by neutral chelate resins or neutral polymer ligands. In these systems, metal atoms or ions are sequestered within such structures as crown ethers, for example, which have been incorporated into the polymer chain. Many reviews of this topic already exist [32]. Another general area of polymer-metal research, which has been explored to a lesser degree, includes mate-

rials which can be considered composites - polymer film-metal laminates and metal-filled polymers. The former situation involves the vapor deposition of metal onto polymer films for the purpose of producing electrically conductive films. The use of inorganic filler particles in preformed polymers has received a growing amount of attention. Adhesive studies with polyimides have been conducted in which the resin contained 5-40% metal or metal oxide filler; enhanced adhesive properties with titanium adherends have been noted [33]. More recently, Bott [34] reported increased lap-shear strengths for polyisoimides loaded with aluminum alloy filler. The final category of polymer-metal systems consists of neutral polymers to which have been added dissolved metal salts, metal complexes, organometallic compounds, or metals. This area has probably received the least study and the work described by this thesis falls into this category.

b. Studies of Polyimides Modified With Dissolved Metal Compounds

Studies in the area last mentioned in the preceding section had their beginnings approximately 30 years ago when Angelo [35] patented a synthetic procedure for the addition of metal ions to several types of polyimides. The goal of this work was to form particle-containing (< 1 μm) transparent polyimide shaped structures, for use as decorative or electrically conductive tapes and packaging materials. The process employed by Angelo involved forming the polyamic acid, dissolving the metal compound in the polyamic acid, shaping the mixture and converting it to the metal-containing polyimide. The properties of one polyimide film were given, which had been cast from a solution of 4,4′-diaminodiphenyl methane and pyromellitic dianhydride (PMDA) in DMF doped with bis(acetylacetonato)Cu(II) ($Cu(acac)_2$). No information was given regarding adhesive properties, T_g , thermal stability, surface resistivity, thermal conductivity, and structures and distribution of the metal-containing precipitates.

Ten years later a report [36] appeared concerning the incorporation of silver into the polyamic acid derived from PMDA and 4,4′-oxydianiline (ODA). Both Ag and $Ag(C_2H_3O_2)$ were utilized, and films containing 0.25-1.00 gram-atom of Ag per polymer repeat unit were obtained. Thermal

and electrical conductivities were increased 3-7 times for the PI film containing dispersed Ag metal, but no changes in these properties were noted for the film containing $Ag(C_2H_3O_2)$. Six years earlier a U.S. patent had been filed for similar work [37]; in this case, the Ag-containing polyamic acid was converted to the polyimide and Ag metal by heating at 300°C under vacuum for 30 minutes. The resulting PI film was described as being tough, flexible, and opaque, though not electrically conductive; however, further heating in air at 275°C for 5-7 hours rendered it conductive, although no resistivity data were reported.

After several more years a technical brief from the National Aeronautics and Space Administration (NASA) described some work involving the incorporation of lithium into polyimides [38]. Superior antistatic properties were reported for a soluble polyimide (DAPI-Polyimide) film loaded with $LiNO_3$ or LiCl. Physical properties and film smoothness remained unchanged, but electrical conductivity was increased about 20-fold over the unfilled polyimide. Additional tests showed that the films were slightly hygroscopic in the presence of lithium ions; this phenomenon was suggested to account for the lowered resistivity. It was not specified whether the enhancement of conductivity was in surface or volume conductivity.

Simultaneous with the above work, a study by Taylor *et al.* [39] was reported involving polyimides derived from 3,3′,4,4′-benzophenone tetracarboxylic dianhydride (BTDA) and diaminobenzophenone (p,p′-DAPB) in DMF, DMAc, and diethylene glycol dimethyl ether (Diglyme) solution. Seventeen different metals in a variety of forms were added to the polyamic acid solutions; in many cases it was possible to cast films and thermally convert the polymer to the corresponding polyimide. Of the films, those that were non-brittle were subjected to thermomechanical analysis (TMA), thermogravimetric analysis (TGA), weight loss on prolonged heating and infrared (IR) analysis. Results of these measurements for a few example systems showed increases in T_g and improved adhesive lap shear strength at 275°C with titanium adherends. However, decreases in TGA polymer decomposition temperature were noted for metal-doped polymers with respect to the corresponding neat polyimides. Predictive trends with particular polymers were not possible.

The effects of metal compound addition on the polyimides' properties depended critically on the choice of metal, its chemical state and its counterion. For example, in certain cases the addition of $AlCl_3$, $AlCl_3 \cdot 6H_2O$ and $Al(NO_3)_3$ apparently caused immediate crosslinking of the polyamic acid such that no film could be cast. Other problems encountered included failure of the metal compound to dissolve in the polyamic acid solution and precipitation of the polyamic acid upon addition of the metal complex. No changes in chemical functionality in the polyimide were apparent from IR spectral comparisons of doped and undoped films, regardless of the metal employed. Continuing work by the same investigators [8,9] included surface and volume resistivity measurements of doped films, X-ray photoelectron spectroscopy, Auger electron depth profiling of film surfaces and additional mechanical property measurements. Effects of metal doping on properties were again found to be case-specific. Upon curing, some of the doped polyimide films developed a metallized-appearing surface on the air side of films cast onto glass; the presence of free oxygen in the curing atmosphere appeared crucial to this phenomenon. Lowering of electrical resistivities were noted for several dopants in some polyimide systems; in many of these cases increases in conductivity diminished or disappeared upon thorough drying of the films, indicating a possible role for absorbed water in the conductivity. For each metal-containing film examined by Instron tensile testing and Autovibron, the elastic modulus increased and the percent enlongation decreased relative to the neat polyimide both at room temperature and 200°C. Most of the doped films tested showed decreases in yield strength and tensile strength over the polymer alone at room temperature, but increases in these values at 200°C. Spectroscopic analysis was performed on the surfaces of two palladium-containing films derived from Li_2PdCl_4 (LTP) and $Pd(S(CH_3)_2)_2Cl_2$ (PDS). Analysis revealed that with PDS doping, significant reduction of Pd to the metallic state had occurred during imidization. Angular-dependent XPS examination and Auger depth profiling showed that most of the Pd in the PDS-containing film lay within the first 100 nm of the film surface; after that it dropped off rapidly to a level similar to that of other residual dopant elements (S and Cl). Similar examination of an LTP-doped film indicated a thin layer of predominantly Pd(0) near the surface, beneath which the film contained a homogeneous mixture of Pd(0) and Pd(II) in nearly equal amounts. Similar studies were made of lithium-doped polymers [40], and it

was found that LiCl partially converts to Li_2O owing to reaction with water during thermal imidization. Unlike palladium, "lithium oxide-like" material tended to stay evenly dispersed throughout the film. Additional work with copper-containing films [41] showed migration and precipitation of copper compounds towards the air side of films cast on glass.

Related and more recent studies involving cobalt and copper dopants have resulted in polyimide films with preferential deposition of metal near the air side surfaces of films cast and cured on glass [42-44]. Films with surface resistivities significantly reduced with respect to the undoped polyimides were formed, and it was found that the codoping of a $CoCl_2$-doped BTDA/ODA film with LiCl further decreased surface and volume resistivities and diminished the activation energy for conduction in the material [42].

C. *Adhesive Bonding of Aluminum*

1. Aluminum Surfaces

Aluminum is an element in group III of the periodic table; it is the most abundant metallic element, comprising more than 8% of the earth's crust by weight. It is a chemically active element and is never found free in metallic form in nature. As a metal in pure form it is light, ductile, and lacks strength. Alloying aluminum can significantly improve its strength; high-performance alloys such as 7075 have strengths approximating those of some steels, with about a third the density. Consequently, high strength aluminum alloys find extensive use in industries where strength and weight savings are crucial, such as aircraft manufacture. Aluminum is the most extensively utilized nonferrous metal, and many alloys lend themselves well to conventional metal forming techniques such as extrusion, drawing, stamping, machining, and cold forming. Aluminum is joined by a va-

riety of means, including welding, brazing, soldering, riveting, bolting, crimping, seaming and adhesive bonding [45-47].

The usefulness of aluminum is enhanced by its tendency to form a thin, stable adherent oxide surface that resists corrosion. This oxide layer, if undisturbed, offers excellent protection of the reactive metal between pH 4.5-8.7; outside of this range, dissolution of Al is rapid. Thus, any procedure involving interaction with the surface of aluminum metal is actually interacting with a layer of aluminum oxide, Al_2O_3. The chemistry, morphology, and physical properties of aluminum surfaces depend strongly on the composition of the metal, its chemical environment, and its mechanical environment. Drastic changes in the morphology of the oxide can occur in response to changes in the chemical environment. Aluminum oxides hydrate readily, and this can give rise to complex microstructures of the surface films. Wefers and Misra [48] have compiled an excellent review of aluminum surfaces as well as the chemistry and properties of aluminum oxides and hydroxides in general.

2. Pretreatments for Adhesive Bonding

a. Degreasing

It is usually desirable for a metal surface to be clean and homogeneous prior to the application of an adhesive. In some cases a particular topography of the surface at the microscopic scale will result in significantly improved metal-adhesive bond strength. These factors can be controlled through surface pretreatment. The simplest and most basic pretreatment a metal surface can receive is degreasing. Degreasing of aluminum surfaces is accomplished in several ways, in which a solvent is applied as a rinse or a wipe, or the metal is exposed to a bath of solvent vapor. Degreasing solvents include acetone, methyl ethyl ketone, and low molecular weight chlorinated hydrocarbons;

the preferred industrial technique for aluminum surfaces prior to adhesive bonding is vapor degreasing with trichloroethane.

b. Simple Etches

Aluminum surfaces are also cleaned with alkaline or acidic etches, sometimes preceded by a degreasing step. Such etches or pickles usually involve chemical attack and dissolution of the surface oxide and often the underlying metal as well, to create a clean and smoothly and uniformly corroded surface. Some etches must be followed by a so-called desmutting step to remove a buildup of reaction products. Chemicals used to clean or etch aluminum surfaces include NaOH, H_2SO_4, and HNO_3 [48,49]. A number of commercial preparations and procedures are available. Mechanical cleaning of surfaces - e.g., grit blasting - is certainly feasible as well, but is more effective when used on harder surfaces such as steel and titanium. Such treatment successfully removes surface material, but at the expense of damage at the microscopic level.

c. FPL Etch

With some chemical surface treatments a metal surface can not only be cleaned, but an oxide layer of specific chemical composition, morphology, and properties can be formed which improve the quality of an adhesive joint with the surface. One such pretreatment widely used for aluminum is the so-called FPL etch, originally developed by Forest Product Laboratory in the 1940s [50]. It consists of soaking the aluminum surface in a hot sodium dichromate/sulfuric acid solution followed by a rinse with clean water. This treatment results in the growth of fingers or whiskers on the oxide surface, illustrated in Figure 4(a) [51], which improve adhesion by providing increased surface area and mechanical interlocking [51,52]. There are a number of procedures for creating a porous oxide or microroughness on Al alloy surfaces; Arrowsmith and Clifford [53] have given an excellent review.

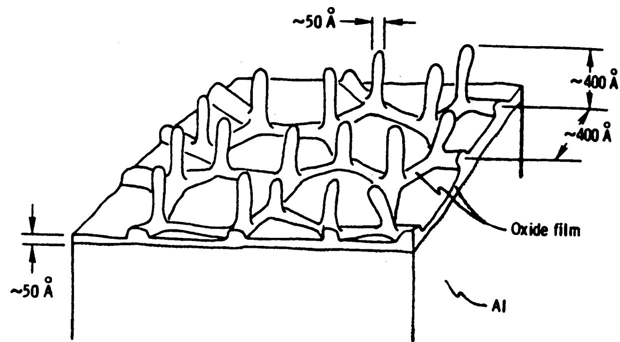

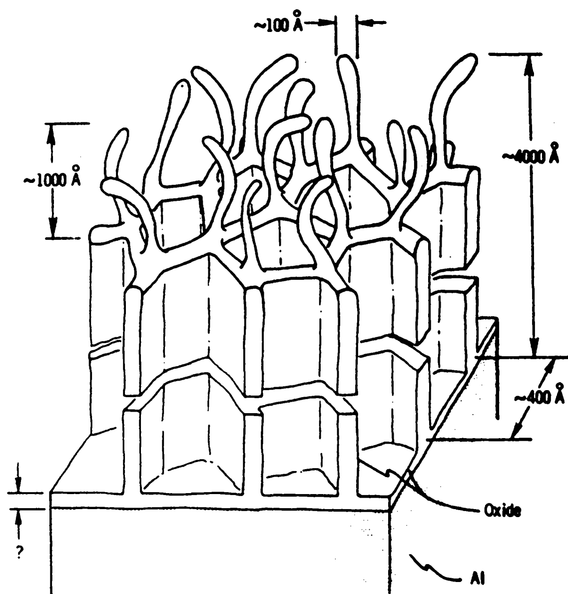

Figure 4. Isometric drawings of oxide structures on (a) FPL etched surface and (b) phosphoric acid anodized surface [51].

d. Conversion Coatings

Other chemical treatments create what are known as conversion coatings. In conversion coatings, the metal oxide is chemically changed, sometimes in discrete layers, to a surface which is intended to encourage chemical interaction with an adherend. These treatments are used prior to the application of lacquers, paints, plastic films, adhesives and lubricants. An example of a conversion coating for aluminum is the chromate-phosphate conversion coating, used to pretreat aluminum sheet to be laminated for structural bonding [49].

e. Anodization

A completely different family of surface film structures with unique properties can be created by combining chemical treatment with electric potential in the process of anodization. Reviews of the subject in the late 1960s and early 1970s [54-56] discussed the morphology and other properties of anodic oxide films, and outline mechanisms proposed to account for their formation. Tajima [56] provides an excellent overview of the history of aluminum anodization and of the varieties of properties engineered into anodic films up to that point, including color, hardness, abrasion resistance, and porosity. Certain anodizing processes provide films which greatly improve adhesion with polymeric coatings and adhesives. Processes which have been most widely studied in this regard include sulfuric acid anodization (SAA) and phosphoric acid anodization (PAA) [7,51,57]. Such anodic films are usually porous and have a columnar cell-like structure, as illustrated in Figure 4(b) [51]. The improvement in performance of many Al-adhesive systems as a result of such anodizing pretreatments is well documented [7,51,57-60].

3. Environmental Effects on Bonds with Aluminum

The study of the effects of environmental conditions on aluminum surfaces and adhesive bond properties is a large subject in itself, and many fine reviews have been offered on environmental attack of metal-adhesive interfaces [60-65]. The worst culprit in environmental attack is generally moisture, and most studies of the subject are concerned with moisture degradation of surfaces and bonds. As stated earlier, aluminum oxide hydrates readily and into a variety of chemical and morphological forms. This behavior can create problems in the durability of an adhesive bond, and in many cases it is beneficial to inhibit the hydration phenomena. Successful attempts at hydration inhibition in aluminum bonds are described by Davis *et al.* [58] and Hardwick *et al.* [59]. Other potentially detrimental effects of moisture on adhesive bonds include plasticization or swelling of the polymeric adhesive by water, hydrolysis or chemical cracking of the adhesive, and effects of water on the thermodynamic interactions of metal and polymer [60-63,65]. Farrar and Ashbee [66] found that soluble impurities present at a glass-epoxy interface can cause the formation of pressure pockets and interfacial gaps due to the ingression of moisture and osmotic pressure. Similarly, Nicholas and Ashbee describe interfacial gaps caused by the freezing of liquid water at an interface [67].

D. Mechanical Adhesion Testing

1. Overview

In order to evaluate the performance of different adhesive-adherend systems under the many conditions to which they are likely to be exposed, a variety of mechanical adhesion tests have been

devised. In most practical cases of engineering, it is not feasible to engage in destructive testing of full-size parts *in situ*, particularly in the case of assessing long-term, time-dependent effects on structures. Thus, standardized laboratory testing procedures are developed and used to compare different bonding situations and to predict the lifetime of a part or material. The American Society for Testing and Materials (ASTM) catalogues and describes experimental procedures for evaluating a wide variety of materials and parts, including adhesive bonds. Mechanical adhesion tests vary significantly in bonding configuration, test conditions, and in how the interfaces are stressed and failed. Brief reviews of adhesive joint test methods appear from time to time [68]; the text by Anderson, Bennett, and DeVries [69] is an excellent compilation of test methods and their numerical analyses.

Probably the test most commonly used is the single lap shear test (ASTM D1002); the specimens are inexpensive, easy to make, and require only a standard tensile test machine to evaluate. Test specimens are bonded in a simple rectangular overlap and then pulled to failure. The highest load achieved, usually in units of MPa or psi, is reported as the lap shear strength. Lap shear strength values are often used to compare the performance of adhesives, but it must be considered that the lap shear configuration does not place the bond overlap in pure shear, owing to the necessity of asymmetric loading of the specimen. There are opening stresses created at the ends of the bond, and the shear stress is not distributed uniformly across the bondline [69]. In addition, the lap shear test is not very sensitive to the surface conditions or pretreatments of the adherends [7], and thus lap shear values are a better reflection of the adhesive's inherent mechanical properties than they are of the nature of the metal-adhesive interface. The Boeing wedge test [70], on the other hand, in which a sharp wedge is driven into the adhesive layer between two bonded coupons, is very sensitive to surface pretreatment. Differences are indicated by different rates of crack propagation from the wedge tip when placed in a specific environment.

2. The Floating Roller Peel Test

Joints are inherently weakest in Mode I loading - tensile opening loads - as compared to Mode II (pure shear) or Mode III (torsional loading). Peel tests are designed to capitalize on this situation by subjecting specimens to high proportions of tensile stress and forcing the entire load to be borne by a narrow strip of the bond. Peel tests are thus very severe tests of the interface being pulled apart.

In general, peel testing consists of pulling, at a constant rate, a flexible adherend off of a rigid substrate to which it has been bonded. Some commonly used peel test geometries are illustrated in Figure 5 [71]. The floating roller peel test (ASTM D3167) consists of placing the specimen in a fixture attached to the crosshead of a testing machine, feeding the flexible strip around the lower roller and into the lower grips of the testing machine, and raising the crosshead at a constant rate to peel the flexible strip from the rigid substrate. The force required to pull this bond apart in this manner is recorded as a function of displacement along the specimen, and is reported as force per unit width of specimen, e.g. N/cm or lb/in.

The test configuration is designed to direct the peeling failure to occur at the interface between the flexible adherend and the adhesive, and unless overshadowed by other factors that is where the failure occurs. The peel force depends not only on the intrinsic strength of the adhesive bond between the adhesive and peel strip surfaces, but also on the rate of peel, the angle of peel, the thickness of the peel strip, and the mechanical properties - i.e., stiffness, viscoelastic properties, etc. - of the adhesive and adherends. The floating roller peel test attempts to keep the angle of peel constant at approximately 116.5°, but since the specimen is not constrained in all directions this constant peel angle is not guaranteed in all cases. For these and other reasons, peel load vs. displacement traces are rarely smooth lines.

Stresses set up in the adhesive layer during peeling have been extensively analyzed theoretically [72 and references therein], particularly by Kaeble [73,74] and Bikerman [75]. Many studies have been reported investigating the effect of peel angle, peel rate, and the thickness of the peel strip on

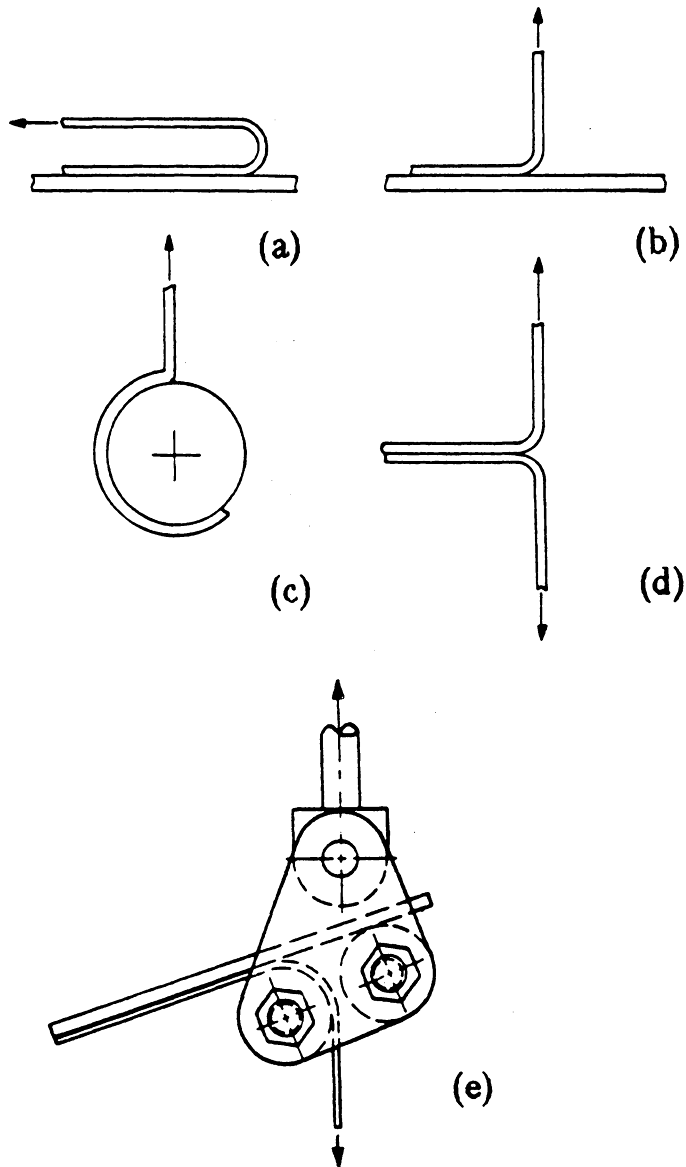

Figure 5. Examples of peel test configurations: (a) 180° peel (b) 90° peel (c) drum peel (d) T-peel (e) floating roller peel [71].

the peel force for many bonded systems. Theories developed to describe the mechanics of peeling, however, were based on the assumption that the flexible peeling adherend remained elastic - that is, experienced no plastic deformation - during the peeling process. This is not the case for peel tests using metallic adherends, like the floating roller test, as the flexible adherend obviously deforms plastically. In addition, the theories do not distinguish the force required to deform the adherend from the force required to fail the bond. In a recent study, Kemp *et al.* [76] analyzed the mechanics of ASTM D3167 and proposed modifications of the test based on their assessment of the method's weaknesses, particularly in the case of weak adhesives with low peel strengths. They modified the test fixture to eliminate unnecessary degrees of freedom for the specimen and to force the peeling specimen to conform to the configuration of the fixture. The results of experiments using this modified fixture supported many aspects of their proposed model and showed that for sufficiently weak bonds, peel load values from unmodified ASTM D3167 tests do not adequately represent the strength of the adhesive-metal interface.

E. Surface Analysis

1. Electron Microscopy

Scanning electron microscopy (SEM) is a technique for obtaining an image of the surface topography of a material at the microscopic level. SEM is widely used in many areas of research, including biology, geology, and integrated circuit development, as well as materials science and adhesive bond studies. The technique offers, especially with modern instrumentation, high resolution and excellent depth of field, which give SEM images their characteristic three-dimensional quality.

In SEM, a focused electron beam, typically at 2 to 30 kV, is rastered over a small area of the specimen's surface; secondary electrons, backscattered electrons, Auger electrons, and x-rays are

emitted from the material as a result. The secondary electrons are detected to form the image displayed on the phosphor screen of a cathode ray tube (CRT). The imaging procedure must take place in a vacuum so that the primary electron beam and secondary electron emission are not significantly attenuated.

Figure 6 [77] is a schematic illustration of basic SEM design. Fundamental components consist of a cathode (electron source), lenses and apertures, electron detector, CRT, a vacuum system, and the requisite electronic controls. An x-ray analyzer is included in the diagram and is a common feature of modern SEM instrumentation. It allows characteristic x-ray emission spectra to be obtained for small features in SEM images, to provide bulk chemical information as well as a topographical image. The electron source for the beam is usually a tungsten filament, which gives off electrons by thermionic emission when subjected to a high potential. The entire apparatus is kept under vacuum not only for imaging, but also to protect the filament, which would rapidly oxidize and fail if exposed to air while hot. The secondary electrons from the specimen are emitted from the top 5 to 10 nm of the surface and are of low energy - usually < 50 eV [77]. The electron detector, a scintillator, is biased so as to accelerate these low energy particles towards the collector at an energy sufficient for detection. Magnification in SEM is simply the ratio of the size of the rastered area on the specimen to the area of the rastered scan appearing in the CRT.

Scanning transmission electron microscopes (STEM) are capable of both SEM and TEM (transmission electron microscopy). When operated in SEM mode, a STEM can achieve higher resolution and magnification than a conventional SEM owing to its higher performance TEM lensing system. Rather than simply being accelerated toward the detector, in a STEM the secondary electrons are made to travel in a helical path through lenses toward the detector. In addition, a STEM operates with a shorter working distance between the electron source and the specimen, resulting in less spreading of the electron beam. The difference in these arrangements is illustrated in Figure 7 [78].

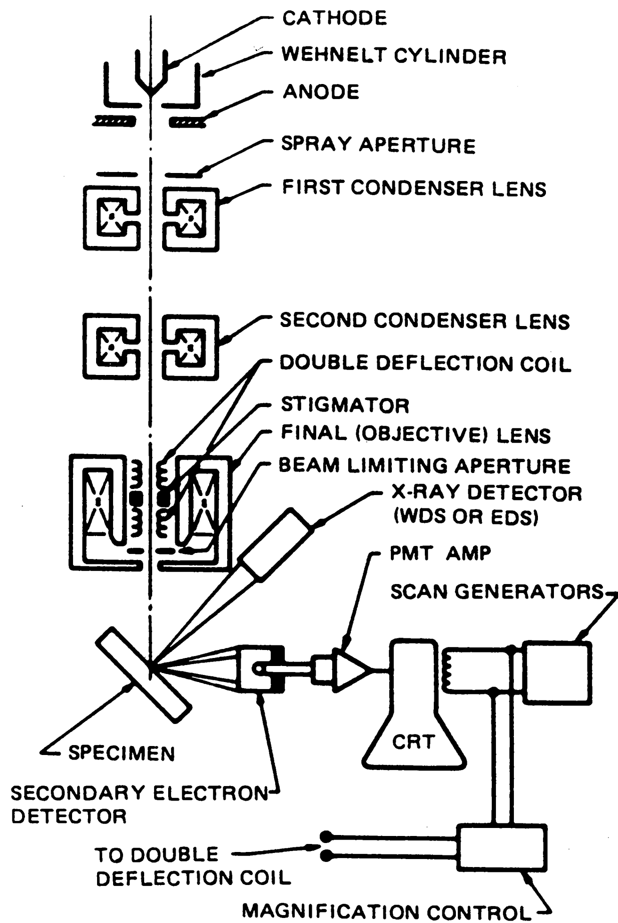

Figure 6. Schematic drawing of SEM instrument [77].

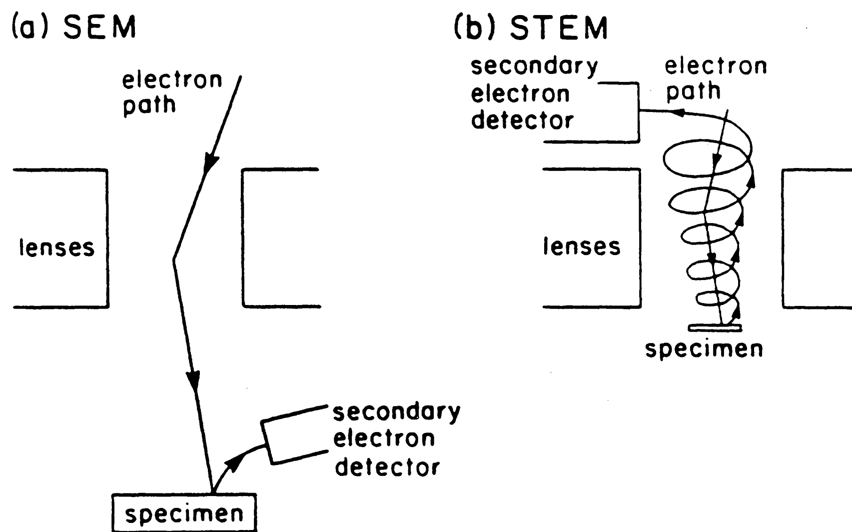

Figure 7. Secondary electron detection system for (a) SEM and (b) STEM [78].

2. X-ray Photoelectron Spectroscopy

XPS is a relatively recent addition to the broad field of materials analysis technology. Developed by Siegbahn and coworkers in the mid 1960s [79] and termed ESCA (Electron Spectroscopy for Chemical Analysis), XPS has become a reliable, refined, and widely used technique for investigating the chemical nature of surfaces. The development and application of XPS and other surface analysis techniques to adhesion studies over the past decade have resulted in major contributions. The ability to probe the chemistry of a surface has allowed the accurate identification of the locus of failure and the direct study of the nature of bonding at interfaces [80].

Simply stated, XPS analysis consists of irradiating a specimen with soft x-rays and analyzing the energies of the resulting photoelectrons emitted. X-ray photons "knock out" electrons from the atoms in the sample, from core levels as well as valence levels. However, only photoelectrons from atoms within 5-10 nm of the surface can successfully escape the material to be detected and analyzed. The entire procedure is performed under vacuum for the same reasons as electron microscopy. A simple illustration of the process is shown in Figure 8 [81].

Each element has a unique photoelectron signature - for a given photon source - due to the unique combination of energy levels available to the electrons in the atom. From the known energy of the incident radiation $h\nu$ and the measured kinetic energy of the emitted photoelectrons $K.E.$, the binding energy $B.E.$ of the electrons is calculated:

$$B.E. = h\nu - K.E. - \phi \qquad [II.7]$$

where ϕ is the work function of the spectrometer. Photoelectron intensity is plotted as a function of either kinetic energy or binding energy to obtain a spectrum. From the relative heights and areas of the photopeaks, quantitative or semi-quantitative information can be obtained. Peaks in the spectrum appear at energy values corresponding to particular orbitals of atoms in the specimen surface. The most commonly used x-ray sources for XPS work are the $K_{\alpha 1,2}$ emission lines of Mg

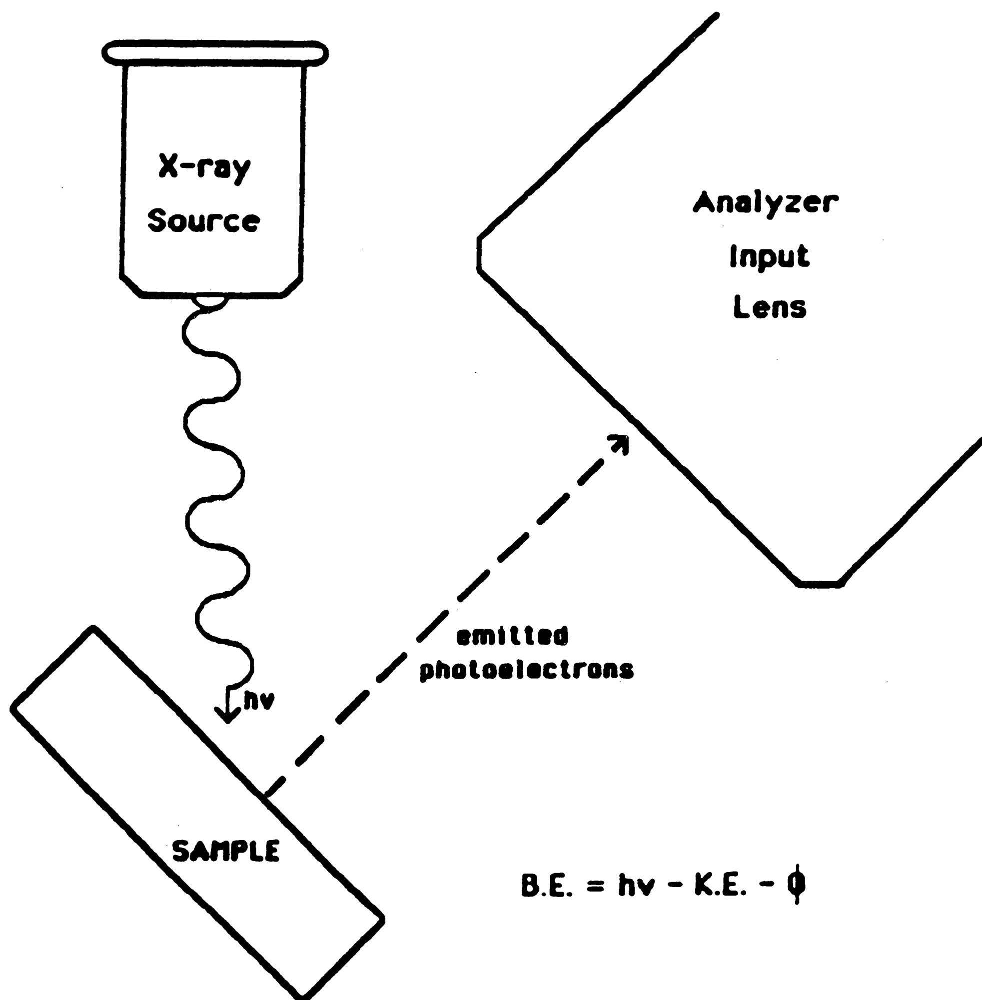

Figure 8. Schematic diagram of XPS analysis [81].

at 1253.6 eV and Al at 1486.6 eV. The linewidths of these sources are 0.70 eV and 0.85 eV, respectively [82-84].

Static charging of the specimen often occurs and can result in broadening or splitting of photopeaks. One widely used method for the calibration of photopeak location is to use the C 1s binding energy from adventitious carbon as a reference, which for this purpose is considered invariant. It has been pointed out, however, by Swift [85] and by Kohiki [86,87] that the precise binding energy value for adventitious carbon can be unclear due to extra-atomic relaxation effects and contamination thickness effects. It was found that the C 1s peak location can vary as a function of the substrate material, depending on its relative ionicity or covalency.

In addition to photoelectrons, Auger electrons are also produced as a result of x-ray bombardment. When an atom is ionized by the removal of an electron from an inner orbital, the atom may "relax" by means of an electron from a higher orbital "jumping" down into the hole in the inner orbital. The energy released from this process may cause another electron to be ejected from the atom. These ejected electrons, called Auger electrons, are usually relatively few in number compared to photoelectrons, but there is often enough Auger emission to cause peaks in XPS spectra. With certain elements an Auger peak can be more intense than the most intense XPS peak, as in the case of sodium. Some Auger peaks coincide with certain XPS peaks on the energy axis, distorting the shape and/or intensity of the XPS peak. Such overlays may be resolved by using an x-ray source of different energy ($h\nu$) [82,83].

The primary source of chemical information in XPS, aside from the relative peak intensities and areas, is the shift in a peak's binding energy due to the effect of chemical interaction on an atom's energy levels; i. e., the involvement of an atom in a chemical bond will be reflected in the binding energies of the atom's electrons. Generally speaking, the more positive the charge on an atom, the more difficult it is to remove an electron, and the higher its binding energy. There is a predictive model for calculating binding energies called the Self Consistent Field method, which is based on the so-called Koopman approximation [82,83]. These binding energy shifts generally range from negligibly small to a few eV - very small in comparison to the magnitude of the binding energies themselves. Thus, the relative positions of photopeaks can reveal to a certain extent the

types of bonding and oxidation states present near the surface of a specimen. Such interpretation of data is not always easy or straightforward, as there are a number of phenomena in XPS which can affect the location, shape, and intensity of photopeaks. These processes include photoionization cross-sections, atomic relaxations, shake-up and shake-off processes, Coster-Kronig transitions, inelastic mean free path of electrons, core vacancy lifetime, spin-orbit coupling, multiplet splitting, specimen charging, and x-ray source anode crosstalk. In-depth discussions of these and other phenomena can be found in a number of texts, articles, and reviews on XPS analysis [82-84,88,89].

III. Experimental Approach

A. Materials

1. Aluminum Adherends

The metal substrates used in this adhesive bonding study were aluminum and aluminum alloys. The rigid adherends or coupons used for the floating roller peel test specimens, 15.24x2.54 cm, were cut from 3.175 mm (1/8″) thick rolled plate of several high strength Al alloys. These alloys vary in composition but all have high strength and stiffness and high-performance applications. The different coupon materials used were Al alloys 2024 (Al-4.4Cu-1.5Mg-0.6Mn), 2090 (Al-2.7Cu-2.2Li-0.12Zr), 6061 (Al-0.6Si-0.28Cu-1.0Mg-0.2Cr), and Alclad 7075 (Al-7.6Zn-2.5Mg-1.6Cu-0.2Cr with low-alloy cladding Al-1.0Zn-0.7Si-0.7Fe-0.1Cu-0.1Mg). Al 2090 was used exclusively as the coupon material in the earliest parts of this study, but was later phased out because of its relatively ″messy″ oxide surface. This light, stiff Li-containing alloy is known to have a thick and heterogeneous oxide film containing a variety of reactive compounds [90]. It was thought that the Li alloy surfaces would not remain stable with time except in an inert

environment, and that more reproducible bonds could be obtained from the comparatively cleaner and more stable surfaces of the more conventional alloys. The flexible adherends or peel strips were cut from 0.1 mm (0.004") thick 99.99% pure aluminum foil.

2. Polyimide Adhesive System

The dianhydride/diamine monomer system used for the adhesive was 3,3′,4,4′-benzophenone tetracarboxylic dianhydride (BTDA) and 1,3-bis(*m*-aminophenoxy)benzene (APB). These monomers and the polyamic acid and polyimide formed from them are illustrated in Figure 9.

The metal-containing dopant salts used in the adhesive were tris(acetylacetonato)Al(III) ($Al(acac)_3$) and anhydrous $CoCl_2$. In previous experiments with BTDA/APB, $Al(acac)_3$ had not been demonstrated to segregate within films cast on glass [91], but it was thought that the compound might do so in an adhesive bond with aluminum and provide a graded interface containing particles of $Al(acac)_3$ or perhaps aluminum oxide. $Al(acac)_3$ was phased out early in the study, after preliminary experiments failed to demonstrate an improvement in peel strength as a result of its addition; in some instances peel strength decreased. $CoCl_2$ had been shown to segregate towards the air side of cast films, and in most cases to partially or completely convert to Co_3O_4 [91]. $CoCl_2$ as a dopant also allowed more meaningful XPS analysis, since the metallic component of the doped adhesive could be easily distinguished from the metal adherend.

Preparation of a typical BTDA/APB batch, enough for 4 peel test specimens, took place at room temperature. Eight mmol APB and 15 ml DMAc were added to a small nitrogen-purged round-bottomed flask and stirred at 150 rpm until dissolved. Next, 8 mmol BTDA was added with 8 more ml of solvent. This solution was stirred at 150 rpm for 3 hours, at which point any needed dopant was added in solid form. The solution was stirred an additional hour at 150 rpm and refrigerated until ready for use. Immediately prior to application, the solution was centrifuged at 1700 rpm for 5 minutes. BTDA/APB is a relatively low T_g polyimide - *ca.* 195-200°C. Thermal imidization - a full cure - is achieved by heating through 300°C.

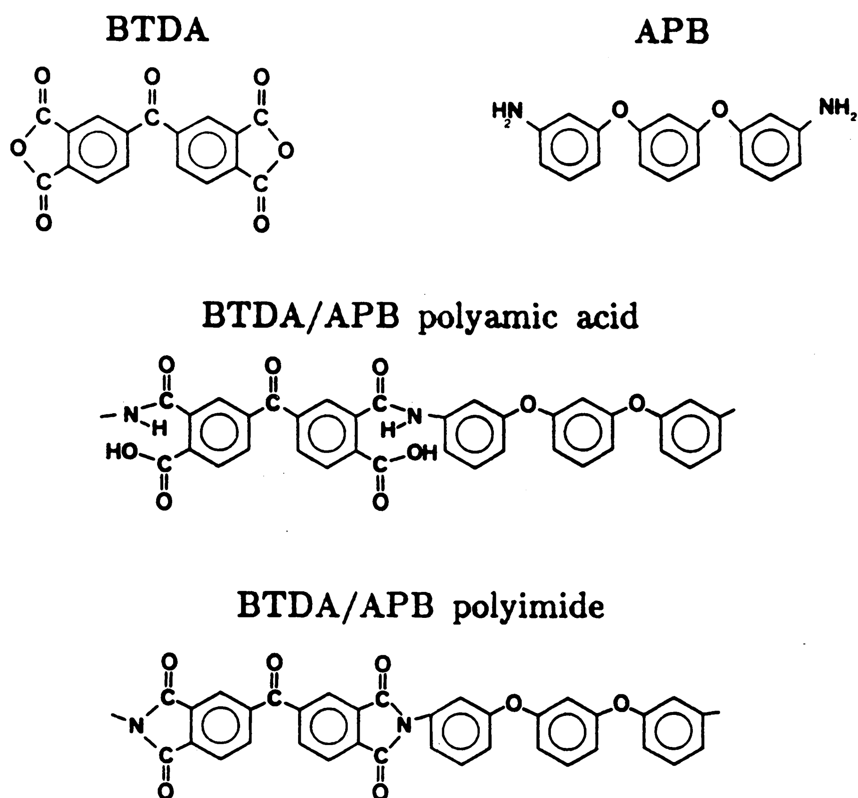

Figure 9. Polyimide system used in this study.

B. Specimen Preparation

1. Surface Pretreatment

To prepare the aluminum surfaces for adhesive bonding, three different techniques were employed - degreasing, an acidic etch, and an alkaline etch. Degreasing originally consisted of an acetone rinse, but later surfaces were wiped as well as rinsed. The acidic etch used was the FPL etch. The etching solution contained 25 g $Na_2Cr_2O_7$ and 55 ml concentrated sulfuric acid in 300 ml deionized (DI) water, and was heated to 75°C. Degreased aluminum surfaces were immersed in this solution for 9 minutes with mild agitation. Specimens were then removed, rinsed with 80°C DI water, and allowed to air dry. Alkaline etching of specimens involved treating the degreased aluminum in a stirred 5% (w/w) aqueous NaOH solution at 55-65°C for approximately 3 minutes for the coupon material and 20 seconds for the foil. Specimens were then washed in a 50/50 (w/w) DI water/concentrated nitric acid solution, rinsed with running DI water, and allowed to air dry. All specimens were stored in a desiccator until use.

2. Peel Test Specimens

a. Application of Adhesive

Application of the adhesive to the adherend surfaces was accomplished by pouring the centrifuged polyamic acid/DMAc solution onto the adherends, drawing the layer on the coupons with a doctor blade set at 0.508 mm and the layer on the foil with a straightedge having 0.254 mm wire spacers, and pre-curing or drying the separate coupon and foil films in a forced-air oven to drive off the solvent. The dried thicknesses of the cast films were approximately 0.0254 mm on the

foil and 0.0508 mm on the coupons. The pre-cure cycle for the first peel specimens in the study was 1/2 hour at 80°C followed by 1 hour at 120°C and 1 hour at 175°C. Later this procedure was adjusted to 1/2 hour at 80°C, 1 hour at 100°C and 1 hour at 200°C, followed by an optional step of 1 hour at 300°C to fully cure the adhesive layers. For a typical batch of 4 specimens, the polyamic acid solution was cast on a single sheet of foil approximately 15x20 cm, and on the 4 coupons. After drying, the adhesive-coated coupons were placed adhesive side down on the sheet of adhesive-coated foil. This batch of specimens was then placed in a heated hydraulic press to bond the foil to the coupons. After the bonding cycle, the four peel test specimens were cut from the sheet of foil. Figure 10 illustrates aspects of the adhesive application procedure.

Several combinations of adhesive layering and doping were used in this study for different experiments, described in more detail later. These bonding configurations are shown schematically in Figure 11.

b. Bonding Procedure

The variables of time, temperature and pressure in stages of the thermal pressing cycle were adjusted somewhat in preliminary experiments in attempts to optimize specimen preparation. The earliest specimens were bonded with the following cycle: heat to 200°C at contact pressure in the press, apply 1.38 MPa (200 psi) and hold for 1 hour, heat to 280°C and hold for 1 hour, and let slow cool under pressure. Subsequent bonds were pressed at 3.45 MPa (500 psi) to improve adhesive-adherend contact. In addition, later specimens were taken through a full cure during bonding and heated through 300°C instead of 280°C in the last step. All specimens were aged in a desiccator for 1 week prior to testing. Bonding procedures for individual experiments are detailed in Chapter IV.

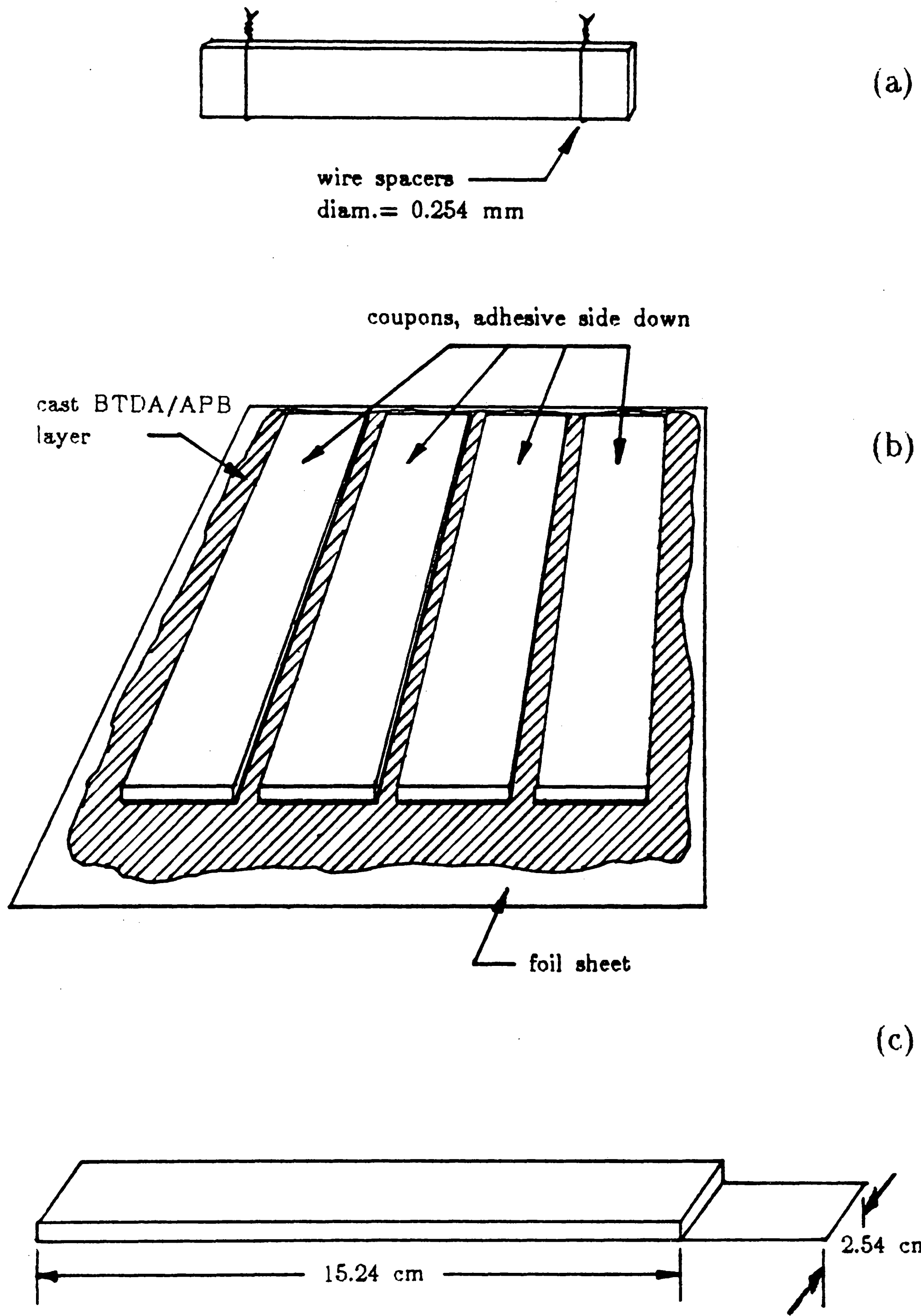

Figure 10. Illustrations of specimen preparation: (a) straightedge for drawing films (b) one batch ready for bonding (c) completed peel specimen.

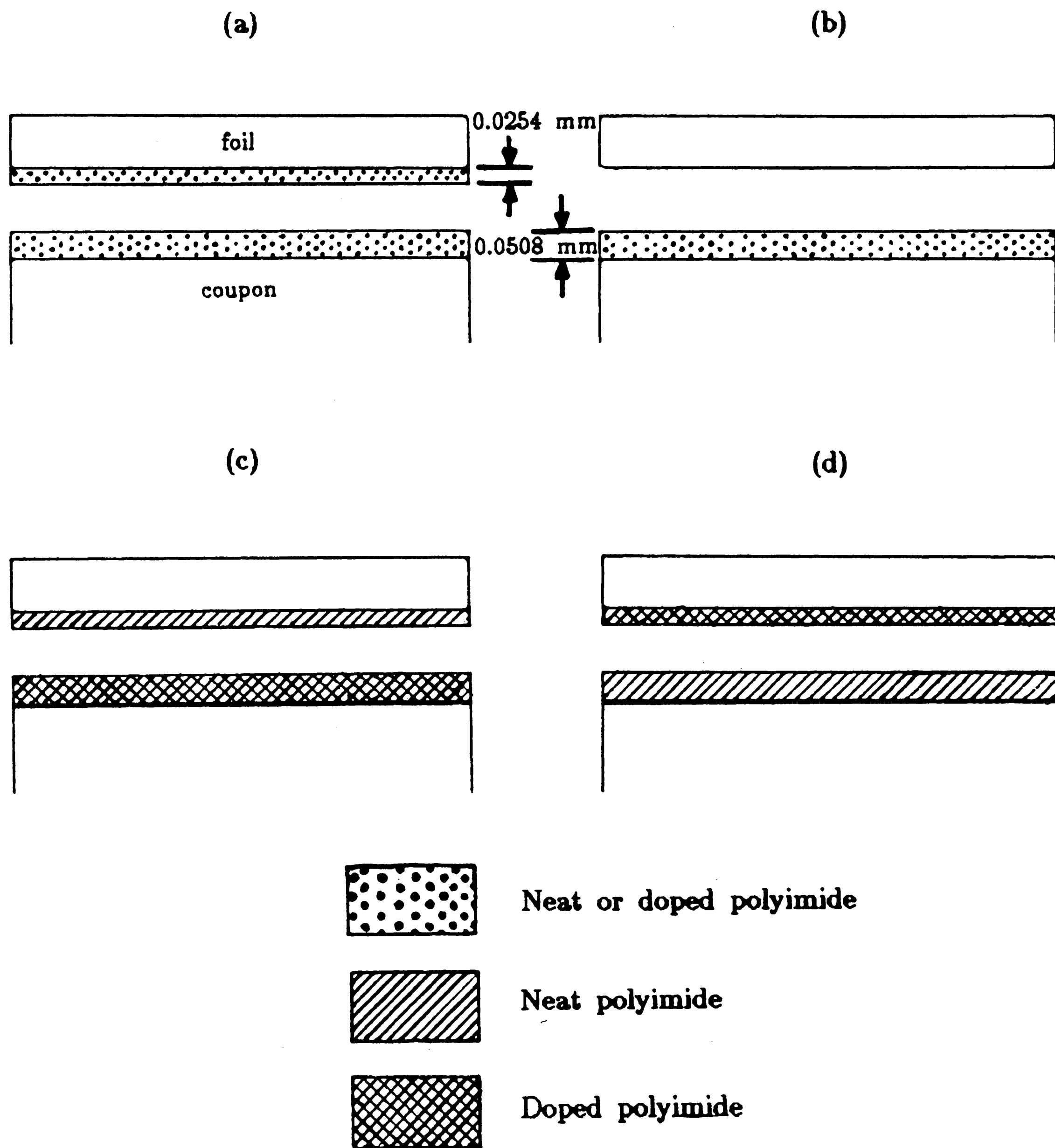

Figure 11. Diagrams of bonding configurations: (a) Coupon layer + foil layer (b) coupon layer only (c) doped film on coupon (d) doped film on foil.

3. Surface Analysis Specimens

Small specimens about 1 cm square for SEM and XPS were cut from coupons with a hacksaw and from foil with scissors. Metal adherend specimens were cut, degreased, and then etched if necessary. Failed peel specimens were stored in a desiccator until having samples cut for examination; care was taken to avoid touching or damaging any surfaces slated for surface analysis.

C. Peel Testing

1. Variation of Peel Rate

Specimens were peeled on an Instron Model 1123 machine controlled by an IBM PC-XT running Instron software under PC-DOS. Typically, a batch of 4 specimens was peel tested for each condition listed, and the peel strength value reported represents the average for the batch. Early in the study peel testing took place at a rate of 0.508 cm/min (0.2 in/min). Tests were time-consuming at this rate, and a few specimens were tested at 1.27 cm/min (0.5 in/min) to see how the faster rate affected the peel load. No significant change in peel strength was noted as a result of this variation. A number of studies - Gent and Petrich, for example [92] - indicate that the spectrum of peel rates over which the peel strength varies substantially is rather broad and ranges over several orders of magnitude of peel rate. Consequently, a change from 0.508 cm/min to 1.27 cm/min would not be expected to show large differences in peel strength. A series of 16 undoped specimens were tested, 4 at each of 4 peel rates: 0.254 cm/min, 1.27 cm/min, 5.08 cm/min and 25.4 cm/min. Average peel strength was found to increase somewhat with peel rate, from 4.9 N/cm at 0.254 cm/min to 9.6 N/cm at 25.4 cm/min. However, this increase in average load was accompanied by

a large increase in the "noisiness" and fluctuation in the plot of peel load vs. displacement. All subsequent specimens were tested at rate of 1.27 cm/min.

2. Elevated Temperature Testing

Several different batches of peel test specimens, prepared with slightly different pre-curing and bonding procedures, were tested at a number of temperatures ranging from room temperature through 205°C. An Instron environment chamber was used with the testing machine, and set with an Instron Model 3116 temperature controller. Most of the specimens so tested were prepared using undoped BTDA/APB, in order to establish a baseline behavior to which the doped adhesive could be compared. The performance of the peel specimens near the T_g of the polyimide was of particular interest, and the greatest number of tests was conducted in the range of 175-205°C. It was expected that peel strength would begin to drop off rapidly at temperatures above the T_g , and that the doped polymer would maintain strength to a higher temperature owing to the T_g-elevating effects of metal compound addition mentioned in the preceding chapter.

3. Variation of Dopant Concentration

An experiment using two different coupon materials, Al alloys 2090 and clad 7075, was conducted in which different amounts of $CoCl_2$ were incorporated into the polyimide. The concentration of $CoCl_2$ dopant added to the polymer was varied from zero through 0.05X, 0.1X, 0.5X, and 1.0X. The designation "X" here represents a dopant concentration such that 1X = 1 mmol dopant per 4 mmol polymer repeat units. This range of dopant concentration is rather broad and it was hoped that an optimum dopant level for this adhesive system would be indicated within it.

4. Effects of Pre-cure Temperature and Surface Pretreatment

In order to reduce the complication and time involved in the process of making specimens, many of the experiments conducted early in this study used specimens prepared with adherends which had been merely degreased prior to bonding. Later, most of the specimens were alkaline etched, as this was found to result in higher peel strengths. A study involving the systematic variation of pre-cure temperature, surface pretreatment and $CoCl_2$ concentration was undertaken. The location of the added dopant was also varied. Specimens using undoped adhesive were compared to specimens in which the doped layer had been cast on either the coupon or foil only, with the other adhesive coat in both cases remaining undoped. This was done in order to establish to what extent the $CoCl_2$ migrated toward the foil-PI interface. Specimens were prepared using both FPL etch and NaOH etch. The doped adhesive layers were pre-cured to either 200°C or 300°C; the undoped layers were taken only through 200°C. Dopant concentrations used were 0.1X and 1.0X; in the undoped control samples, the coupon layers were pre-cured to both 200°C and 300°C.

5. Environmental Exposure

The effect of hot water exposure on the peel behavior of this system was studied for both undoped and 1.0X $CoCl_2$-doped adhesive. After bonding and the 1-week aging period, specimens were placed in a bath of DI water maintained at 70 ± 4°C. Specimens were removed after intervals of 1, 10, 50, and 100 hours of exposure and peel tested within 30 minutes of removal from the water.

D. *Surface Analysis*

1. SEM

The surface topography of the pretreated foil surfaces were studied using STEM instrumentation. Small pieces of foil were pretreated by acetone wipe, FPL etch and NaOH etch and then sputter coated with gold prior to examination. The photomicrographs were acquired in the SEM mode using a Philips EM-420T electron microscope equipped with a Tracor Northern 5500 EDX image analysis system. SEM images were also obtained of the failure surfaces of peel test specimens. Small samples of the peel specimens were cut and sputtered with gold for imaging. The instrument used was an International Scientific Instruments SX-40 scanning electron microscope.

2. XPS

X-ray photoelectron spectra of the failure surfaces of peel specimens were obtained using a Perkin-Elmer PHI 5300 ESCA system. The x-ray source used for all samples was a Mg anode operated at a power of 250 W; the spot size analyzed was approximately 2x10 mm. The specimen surfaces were not cleaned or sputtered in any way after introduction to the high vacuum chamber; the spectra obtained therefore include any contamination picked up during handling, barring whatever volatile contaminants were stripped off upon exposure to the $\simeq 10^{-8}$ torr vacuum in the analysis chamber.

A survey scan of each sample was obtained over a binding energy range from 0 to 1000 or 1100 eV. Narrow scans were obtained for all significant peaks noted in the wide scan spectra, and for any other elements of interest. Relative atomic percents were calculated from the peak areas of each element using software supplied for the spectrometer computer by Perkin-Elmer.

IV. Results and Discussion

A. *Preliminary Experiments*

1. SEM of Pretreated Foil Surfaces

High-resolution SEM images of Al foil which had been pretreated by acetone wipe, NaOH etch and FPL etch are depicted in Figures 12-14 at a magnification of 50,000X. All three surfaces show different topographies at this level. The acetone-wiped surface appears rather crusty and flaky, with particles on the surface which may be dust or loose pieces of oxide. The NaOH-etched foil has the characteristic cratered and pitted appearance of a corroded surface; the surface within the craters appears bumpy or nodular at a fine scale, *ca.* 0.01 μm. The FPL-etched foil appears to have a network of threadlike structure over a finely bumpy surface, similar to that described by Venables *et al.* [51]. The dimensions of the small bumpy features in this photomicrograph correspond with the approximate diameter of the oxide "fingers" produced by the FPL etch - *ca.* 5 nm. Both the NaOH-etched and FPL-etched surfaces are more highly structured than the simply de-

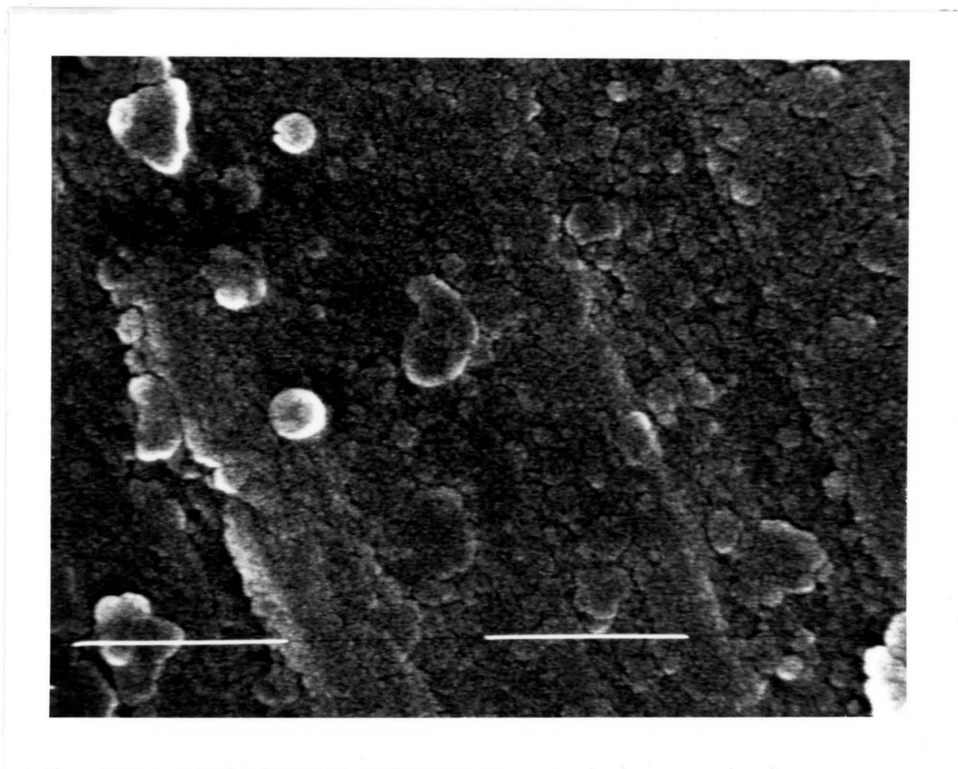

Figure 12. High-resolution SEM of acetone-wiped Al foil surface, 50,000X; white bar = 50 nm.

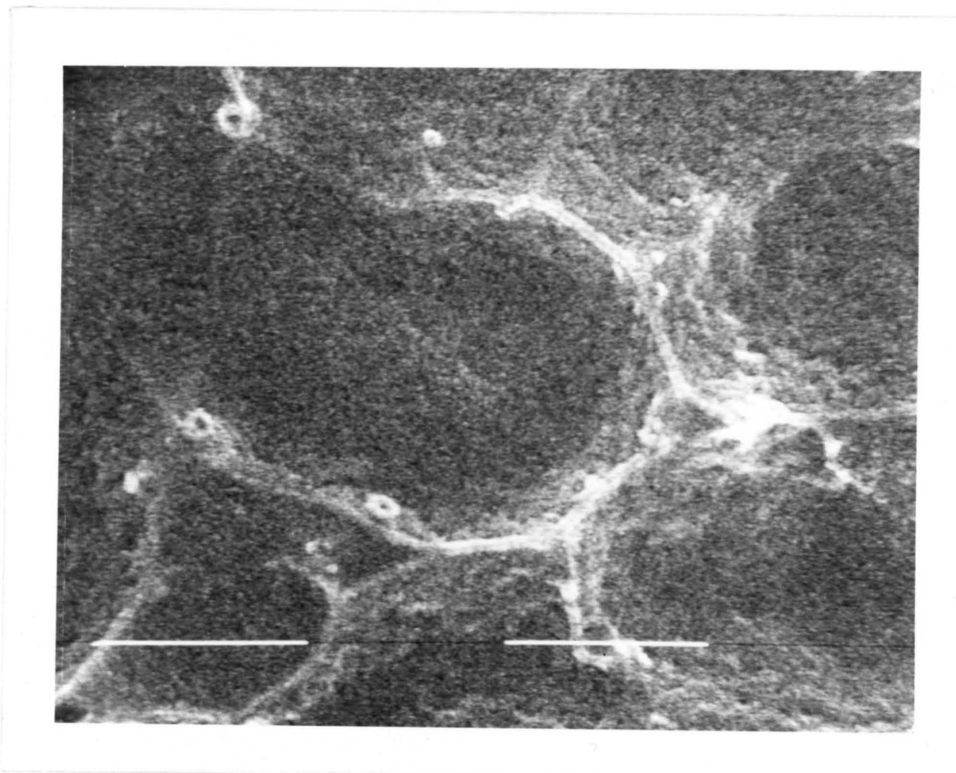

Figure 13. High-resolution SEM of NaOH-etched Al foil surface, 50,000X; white bar = 50 nm.

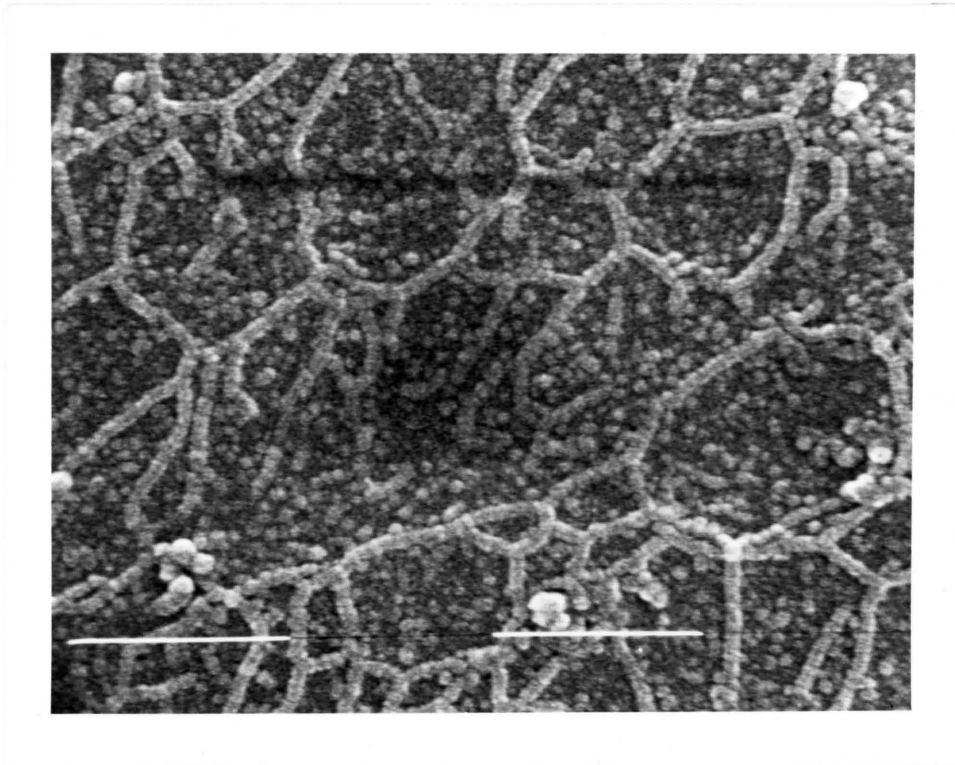

Figure 14. High-resolution SEM of FPL-etched Al foil surface, 50,000X; white bar = 50 nm.

greased surface, and appear more homogeneous; both these factors would generally be considered to promote better adhesion between the foil and adhesive.

2. Single Adhesive Layer Bonds

Since $CoCl_2$ in BTDA/APB was known to segregate toward the air side of films cast on glass [91], it was thought that the dopant might do the same in a film cast on aluminum and that foil then might be directly bonded to the graded surface region. Specimens were prepared in which BTDA/APB films - neat, or doped with either $Al(acac)_3$ 1.0X or $CoCl_2$ 1.0X - were cast on the coupons only and the degreased or FPL-etched foil left uncoated, as shown in Figure 11(b). The adhesive layers were pre-cured through 100, 175 or 300°C. Bonding of the foil to the dried adhesive layers took place at 1.38, 3.45 and 6.90 MPa (200, 500 and 1000 psi) and a maximum temperature of 280°C.

Peel results for the single-layer bonds are not shown; all these specimens bonded poorly and were very weak. In all cases the peel strength averaged 1.8 N/cm or less, and sections of some bonds came apart easily in the hand. For comparison, several batches of specimens were made, under conditions like those described above, in which the foil adherends were primed by casting layers of adhesive on them as well as on the coupons. A batch of specimens using undoped adhesive, a 175°C pre-cure, and a bonding pressure of 1.38 MPa gave an average peel strength of 13.1 N/cm. A similar batch of specimens bonded with $Al(acac)_3$-doped adhesive averaged 5.3 N/cm. The consistently low or negligible peel strengths of specimens in which the foil was not coated with adhesive were attributed to poor interfacial contact between the foil surface and the dried adhesive layer during bonding. The highly viscous nature of the polymer, even when not fully imidized, may have resulted in poorer wetting of the foil surface than was possible with a solution of the polymer cast directly onto the foil. In this experiment, the pretreatment of the foil surface prior to bonding did not have a noticeable effect on the peel stength.

3. Variation of Pre-cure Temperature

The necessity of casting a primer coat on the foil adherend to get a better bond meant that two layers of adhesive had to consolidate into one in order to get a workable peel specimen. Because of the rigid nature of the cured polyimide, it was thought that the two BTDA/APB layers would incorporate into one another less if both layers were fully cured (imidized) before being brought together. On the other hand, the fully imidized polymer was the stronger material and would thus improve the adhesive bond strength.

Two batches of peel test specimens were made with degreased and NaOH-etched adherends and $CoCl_2$ 1.0X-doped adhesive pre-cured to 200°C. Three more batches using degreased and FPL-etched surfaces, and both doped and undoped adhesive, were made in which the coupon layers were fully cured through 300°C prior to bonding. All specimens were bonded at a pressure of 3.45 MPa through 280°C. The results of peel testing are shown in Table 1.

Fully curing the coupon layer prior to bonding appeared to result in a noticeable increase in peel strength for the degreased specimens (5.3 compared to 3.0 N/cm). However, this change was within what was taken to be the standard variation in these peel load measurements - $\pm$2.0 N/cm. It is apparent that even with a fully cured coupon layer, the adhesive consolidated sufficiently well to get acceptable peel results. A significant increase in peel strength was seen as a result of FPL etch (for the undoped polyimide) or NaOH etch (for the doped material) pretreatments over simple degreasing. These findings suggested that coupon layers in later specimens could be pre-cured through 300°C and that etched adherends should be used. The difference in peel strength between the undoped and 1.0X-doped specimens with degreased adherends and pre-cured through 300°C was less than 1 N/cm, within the standard variation.

Table 1. Results of variation of pre-cure temperature.

Pre–cure Temperature	Surface Pretreatment	$CoCl_2$ conc.	Peel Strength (N/cm)
200°C	degrease	1.0X	3.0
	NaOH etch	1.0X	8.8
300°C	degrease	1.0X	5.3
	degrease	undoped	6.1
	FPL etch	undoped	20.1

4. Elevated Temperature Study

At about the same time as the above experiment, four batches of specimens made with undoped adhesive and degreased adherends were peel tested at elevated temperature. Four specimens each were tested at room temperature (25°C), 75, 125 and 175°C. No significant change in peel strength was shown for these temperatures, but at 175°C the average value was higher than the other three. This trend was also seen later when undoped NaOH-etched specimens were tested at higher temperatures. For these specimens, peel strength peaked at 190°C at an average value of 21.9 N/cm and then began dropping off rapidly to 11.3 N/cm at 205°C. Results of these tests are listed in Table 2.

It was surmised that the relatively brittle and rigid polymer gained enough resiliency as it neared its T_g to allow more even distribution of stress in the failing bond, thus causing the observed increase in peel strength. As the T_g was passed, the polymer began to flow so readily as to fail at lower stresses. The peel load vs. displacement traces of failures also changed in appearance, rather abruptly, from a relatively noisy trace below the T_g to a very smooth trace above the T_g. A typical trace of each type is shown in Figure 15.

Another two batches of specimens were prepared using BTDA/APB doped with $CoCl_2$ 0.1X and 1.0X. These were tested at 195°C in order to see whether the doped adhesive would maintain strength to a higher temperature than the undoped material. All of these specimens peeled apart between the two adhesive layers rather than at the foil-adhesive interface (see Table 2), so no useful peel load data were obtained for the interface of interest.

5. Variation of Dopant Concentration

The last study undertaken with degreased adherends was one involving the systematic variation of $CoCl_2$ concentration from zero through 1.0X. One series of specimens used coupons made of

Table 2. Results of elevated temperature peel testing.

Surface Pretreatment	$CoCl_2$ conc.	Test Temp. (°C)	Peel Strength (N/cm)
degrease	undoped	25	6.1
degrease	undoped	75	6.1
degrease	undoped	125	6.1
degrease	undoped	175	7.5
NaOH etch	undoped	25	14.9
NaOH etch	undoped	185	19.3
NaOH etch	undoped	190	21.9
NaOH etch	undoped	195	17.5
NaOH etch	undoped	205	11.3
NaOH etch	0.1X	195	*
NaOH etch	1.0X	195	*

*Specimens failed between the adhesive layers; no useful data.

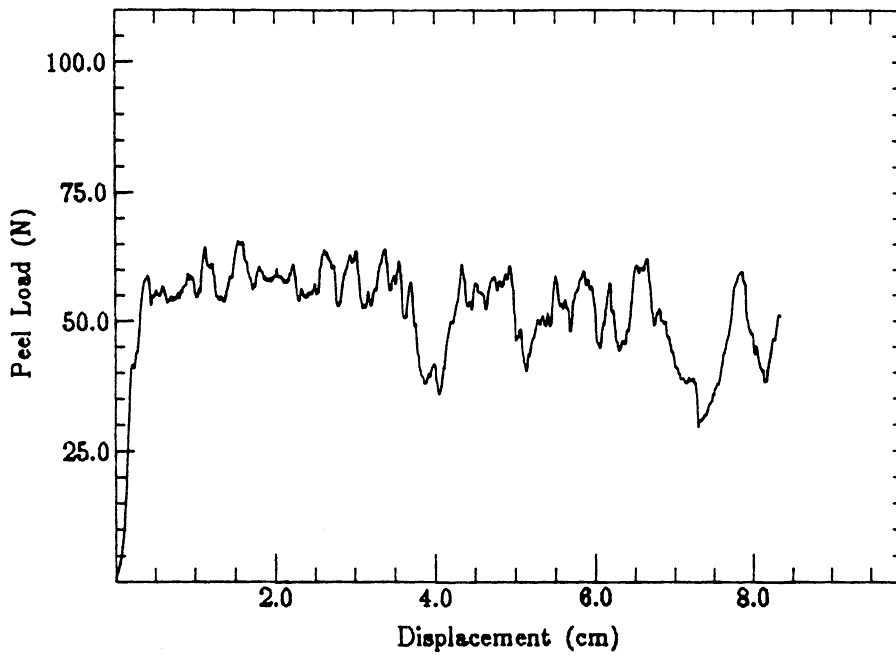

(a)

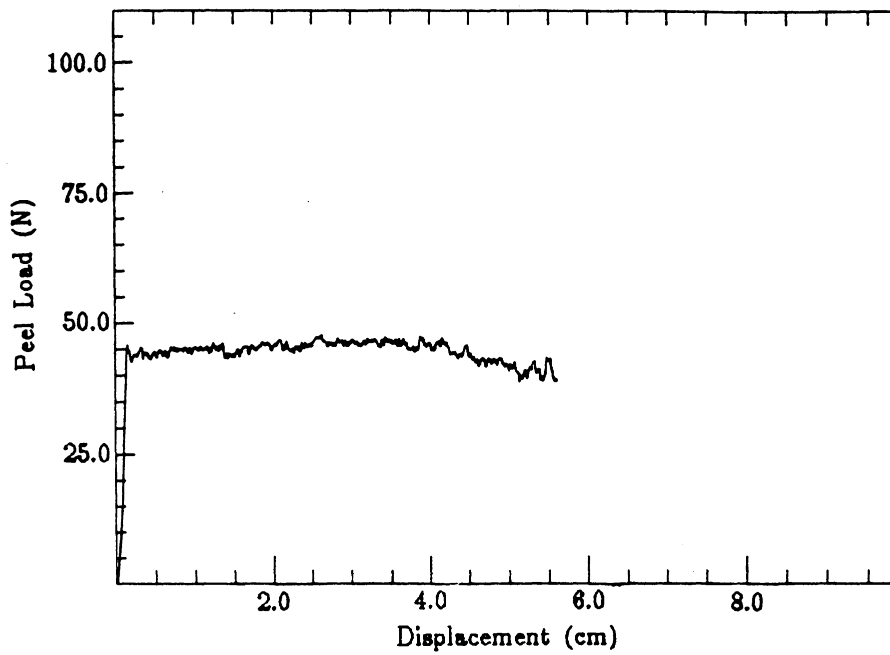

(b)

Figure 15. Peel load vs. displacement plots for specimens tested at (a) 190°C and (b) 195°C.

alloy 2090 and the other using clad 7075. All specimens received the same pre-curing treatment, foil through 200°C and coupon through 300°C, and the same bonding cycle - through 280°C at 3.45 MPa. Peel test results are shown in Table 3.

Overall, no significant variation in peel strength was shown as a function of dopant concentration. Specimens made with alloy 2090 gave slightly higher values and showed a small increase in peel strength with increasing $CoCl_2$ concentration, but the difference was well within the standard variation. These results did not indicate a dependence of peel strength on dopant concentration. It is possible that specimen preparation procedures were not yet optimized and that the bonds were too inherently weak owing to other factors to show differences in peel strength from varying the dopant concentration.

6. Conclusions

Conclusions drawn from the experimental work described above can be summarized as follows:

- casting the adhesive from solution directly onto the foil results in better bonding (see section IV.A.2);

- sufficient consolidation of the two adhesive layers for most peel tests can be achieved when the foil coat is pre-cured to 200°C and the coupon layer fully cured prior to bonding (see section IV.A.3);

- doping of BTDA/APB with $CoCl_2$ has not resulted in consistently higher peel loads at room temperature, but may still be expected to improve peel strength at elevated temperature (see section IV.A.5).

Table 3. Results of variation of dopant concentration.

Coupon Material	$CoCl_2$ conc.	Peel Strength (N/cm)
2090	undoped	6.1
	0.05X	6.1
	0.1X	6.3
	0.5X	*
	1.0X	6.7
7075	undoped	5.3
	0.05X	5.8
	0.1X	5.3
	0.5X	5.1
	1.0X	5.3

*Specimens failed between the adhesive layers; no useful data

Specimens were subsequently prepared to receive a full cure during bonding to see whether a graded interface would form in the doped polyimide against the aluminum surfaces during curing.

B. Study of Doping, Pre-cure, and Surface Pretreatment

1. Peel Test Matrix

Table 4 documents a study in which the dopant level, the pre-cure temperature, the surface pretreatment, and the adherend on which the doped adhesive layer was initially cast were systematically varied with all other paramenters remaining the same. $CoCl_2$ concentrations used were zero (undoped BTDA/APB), 0.1X and 1.0X. The doped adhesive layers were either pre-cured through 200°C or fully cured through 300°C prior to bonding, with the undoped layers always pre-cured through 200°C. Both FPL etch and NaOH pretreatments were used on the adherends, and the doped layer of adhesive was cast on either the coupon adherend or the foil. The bonding configurations used for the specimens described in Tables 4(a) and (b) were those illustrated in Figures 10(c) and (d) respectively. The undoped specimens described in Table 4(c) were prepared as shown in Figure 10(a). All specimens were bonded in the press under the same conditions - through 300°C at 3.45 MPa.

Table 4. Peel strengths as a function of pre-cure, surface pretreatment, and dopant level; peel strength values in N/cm.

(a) Doped Film on Coupon

0.1 X		1.0 X		Dopant Level
200°C	300°C	200°C	300°C	Pre–cure Temperature
12.9	11.0	9.2	15.1	FPL etch
12.3	*	10.0†	*†	NaOH etch

(b) Doped Film on Foil

0.1 X		1.0 X		Dopant Level
200°C	300°C	200°C	300°C	Pre–cure Temperature
10.6	*	2.4	*	FPL etch
9.4	*	2.7	*	NaOH etch

(c) Undoped

200°C	300°C	Pre–cure Temperature
18.9	18.8	FPL etch
16.6	14.0	NaOH etch

* Specimen failed between the adhesive layers; no useful data
† Some debonding occurred between adhesive and coupon

2. Results

a. Pre-cure Temperature

In each case where the doped adhesive coat on the foil was fully cured prior to bonding, the two adhesive coats failed to consolidate and the specimens easily came apart between the adhesive layers, according to the results listed in Table 4(b). It is apparent that full cure of either adhesive layer prior to bonding sometimes results in poor consolidation of the layers during the bonding procedure. The fully cured adhesive is more resistant to flow than the less cured material; even when heated well above its T_g and under pressure, it resists forming one continuous layer of adhesive from two coats. The consolidation problem was more pronounced when doped adhesive was used, particularly when the foil layer was doped. During full curing of the cast adhesive layer, some of the dopant may segregate toward the air surface and possibly act as an obstruction at the adhesive-adhesive interface, limiting interdiffusion between the polymer surfaces. Otherwise, there was no clear trend of peel strength as a function of pre-cure that was outside the statistical variation between individual specimens.

b. Surface Pretreatment

The results described in Tables 4(c) indicate a slight improvement in peel strength due to FPL etch pretreatment vs. NaOH etch when undoped adhesive is used; for the doped specimens the difference was within the standard variation of ± 2.0 N/cm. The FPL etch would be expected to lead to better adhesion to an aluminum surface compared to the NaOH etch because of its greater surface area and somewhat more homogeneous structure [51], but in this particular case any improvement was generally within statistical variation. Differences in peel strength with respect to FPL etch vs. NaOH etch were more pronounced with the undoped adhesive; it may be that the

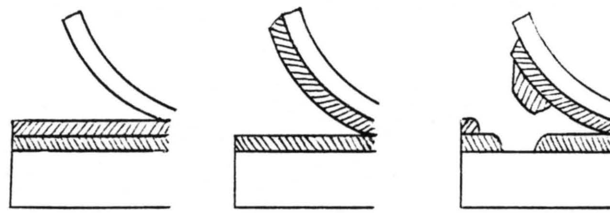

(a) (b) (c)

Figure 16. Photograph of peel specimens, failure at (a) foil-adhesive interface (b) between adhesive layers (c) mixed; some at adhesive-coupon interface.

presence of dopant in the adhesive somehow limits the amount of polymer in contact with the pretreated surface, if segregated dopant material collects at the surface and displaces the polymer. In two cases, using NaOH-etched adherends and $CoCl_2$ 1.0X-doped adhesive cast on the coupons, significant amounts of peel failure occurred at the adhesive-coupon interface. A photograph illustrating the three different types of peel failure seen in this study is shown in Figure 16. Failure at the adhesive-coupon interface indicates a very weak bond between these surfaces - weak enough to cause the failure to shift away from the adhesive-foil interface to which it is directed by the floating roller peel test. This type of failure did not occur in preliminary experiments, and nothing indicative of an explanation for this behavior was noted during the testing. It is likely that the dopant migrated towards the coupon surface as well as the foil surface and became sufficiently concentrated to displace polymer from the coupon surface.

c. Dopant Concentration

The results in Table 4 show that specimens made with undoped adhesive gave consistently higher peel strengths than those made with $CoCl_2$-doped adhesive. In most cases, the lower dopant concentration resulted in higher peel strength values than the higher concentration. In the case of the doped film cast on the coupon with FPL etch pretreatment, however, the peel strength was higher for 1.0X than for 0.1X. Peel strength was decreased for specimens in which the foil layer was doped as opposed to the coupon layer. However, a full set of data was not available as all specimens in which the foil layer was fully cured before bonding failed between the adhesive layers.

It is apparent that the addition of $CoCl_2$ to BTDA/APB polyamic acid did not improve the adhesive strength of a bond to aluminum when tested in this manner. It is possible that the dopant material segregates toward the adhesive-metal interface to such a degree that it displaces polymer from the metal surface and acts as a weak boundary layer. It is also possible that the polymer surface-dopant-metal surface interphase region is stronger in shear loading than in peel loading; in which case a different mechanical adhesion test method, a lap shear method for example, may show

different trends of bond strength with dopant concentration. It is possible that further refinements of specimen preparation procedure - pressure and temperature sequence, for example - may improve overall bonding to the point where more subtle differences in peel strength may become apparent.

3. Analysis of Failed Surfaces

a. SEM

Representative SEM images of failed peel surfaces are shown in Figures 17 and 18. Both specimens failed at approximately the same peel load; the foil sides and polymer sides of these bonds, which were made with NaOH-etched adherends and doped and undoped adhesive, are shown at a magnification of 2000X. The foil surface of a failed specimen made with undoped BTDA/APB, Figure 17(a), is relatively homogeneous. Striations are evident which were not present on the original foil surface and which apparently correspond to fine creases made in the foil during peeling, as well as dust particles. It is not clear in this image whether the surface is bare foil or has a thin film of adhesive remaining. The corresponding polymer side of the same failure shows parallel striations pocked with small drawn-up areas of polymer resembling those caused by viscous failure. Other striations appear on the surface which are not parallel to the peeling creases and which may be replicas of scratches present on the matching foil surface, suggestive of good wetting between the adhesive and the foil.

Figure 18 depicts corresponding foil and adhesive surfaces of specimens made with $CoCl_2$-doped adhesive. The foil side shows areas of bare or only thinly covered metal, with scratches and some small irregular pits or pores in the metal surface. Other areas of the image appear to be patches of thicker polymer film on the foil. In contrast to the undoped specimen, there are wavy, irregular ridges apparent on the surface which suggest uneven debonding of the foil sur-

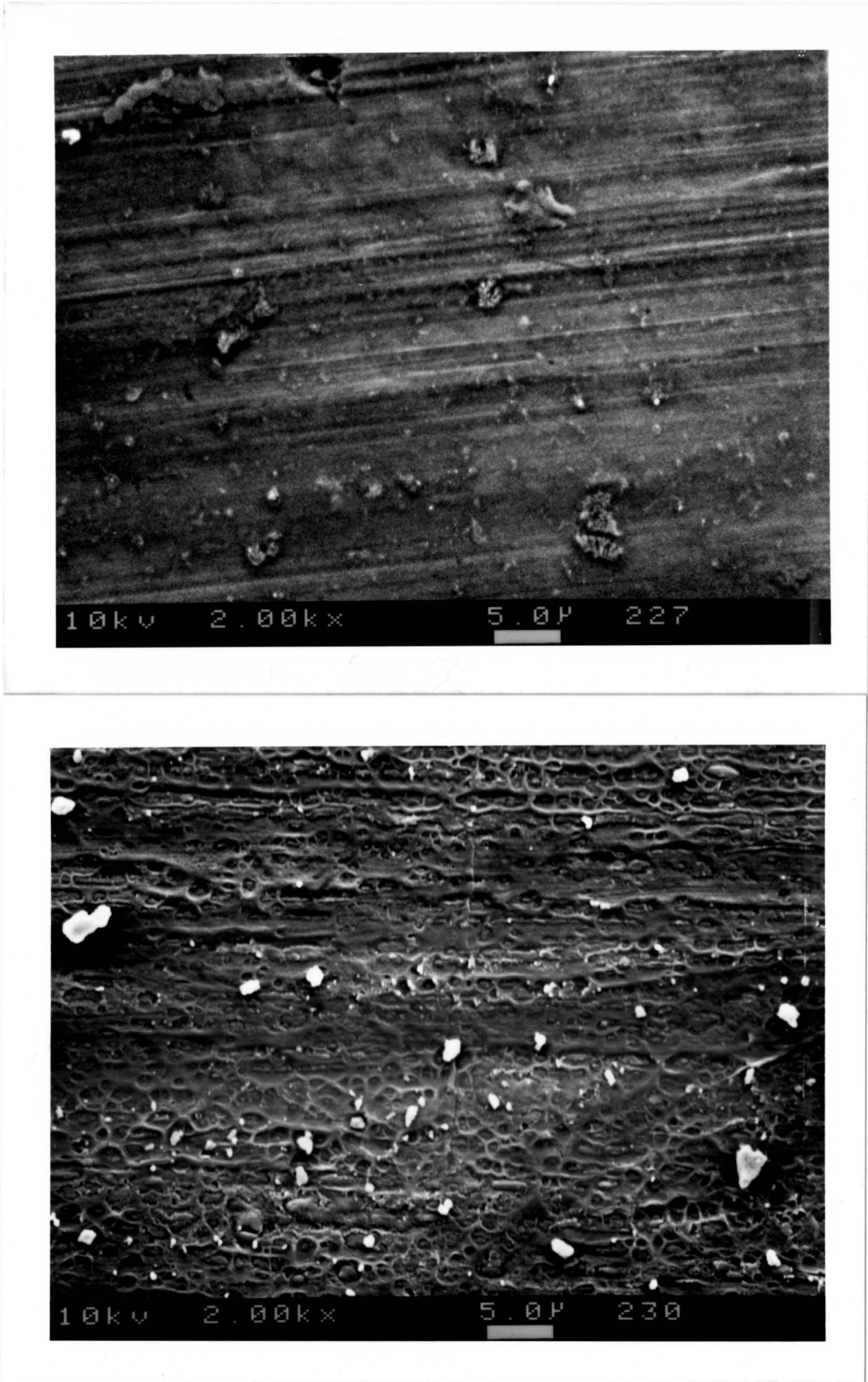

Figure 17. SEM images of failed peel surfaces, 2000X: undoped adhesive (a) foil side (b) adhesive side.

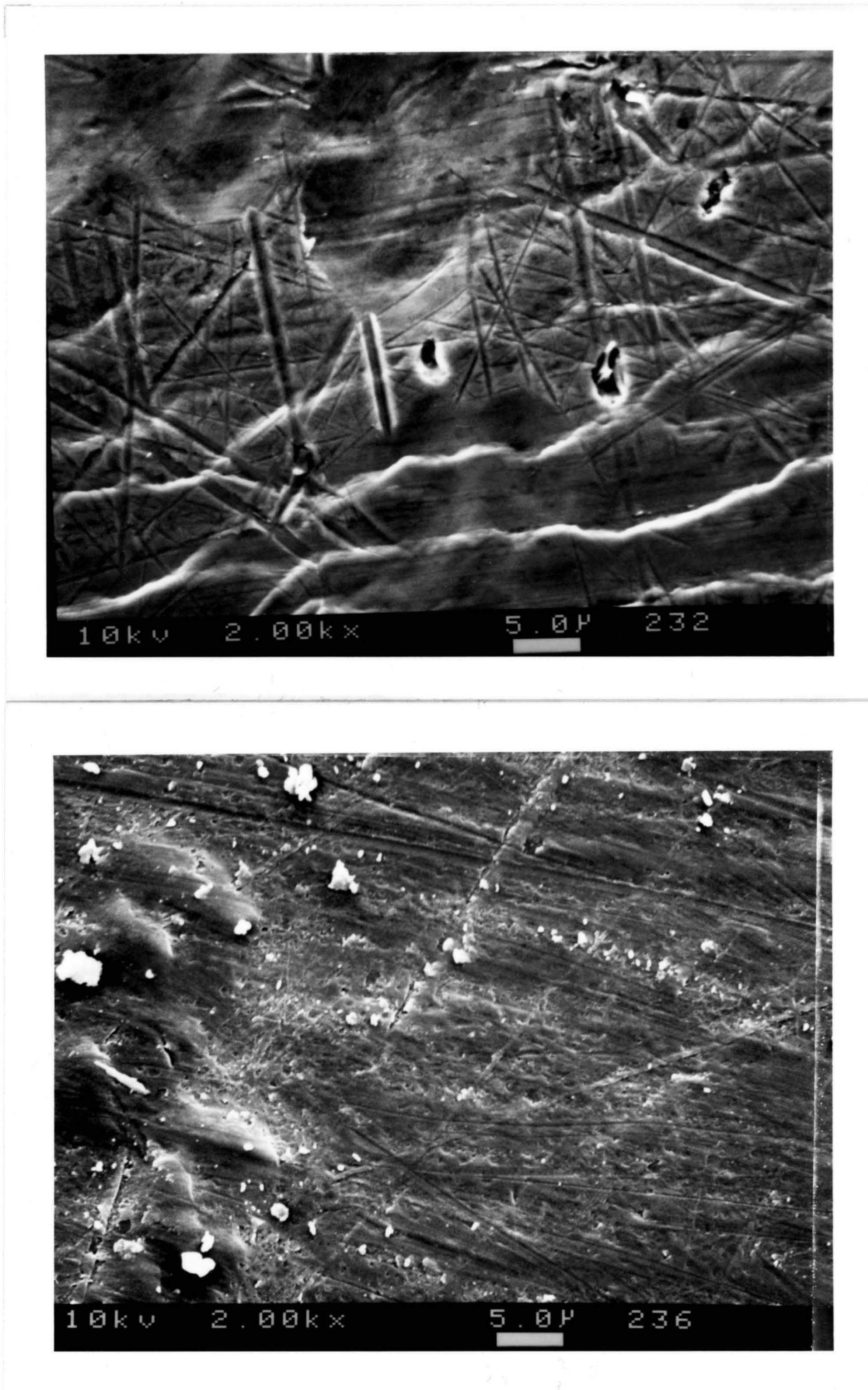

Figure 18. SEM images of failed peel surfaces, 2000X: BTDA/APB//$CoCl_2$ (a) foil side (b) adhesive side.

face from the adhesive at the microscopic level. The polymer side of the failed bond, in comparison to the undoped failed adhesive surface, is relatively smooth except for dust particles and some lumpiness of the surface mirroring etch pits in the foil surface, again suggestive of good wetting. In some areas very small amounts of viscous pulling are evident. The smoothness of the doped adhesive surface in comparison to the undoped material is an indication that the doped material is more rigid and does not flow as much under the stresses imposed during failure. The much smaller degree of plastic deformation sustained by the doped adhesive during failure may account, at least in part, for the lower peel strengths observed for doped specimens. Such plastic deformation as seen on the neat polymer surface dissipates energy and the energy required to deform the polymer is added to the energy required to deform the flexible adherend and the energy required to separate the interface.

b. XPS

Cured adhesive surfaces and the failed surfaces of the peel specimens in the study described in section IV.B.2 were examined by XPS; some of the specimens from preliminary experiments had also been examined. It was consistently found that the failed foil surfaces included thin deposits of polyimide, even when the specimens failed according to the design of the peel test and the foil appeared bare and free of adhesive. XPS C 1s photopeaks obtained from a polyimide surface (an adhesive layer cast on a coupon) and a failed foil surface are shown in Figure 19. The peaks' shapes and binding energy values - setting the main C 1s peak at 285.0 eV - are essentially identical, and as expected for this polyimide system given its molecular structure (see Figure 9). The small peak to the high binding energy side of the main carbon photopeak is contributed principally by the carbonyl carbon atoms in the polymer.

That the polyimide deposits on the failed foil surfaces were either very thin or sparse and patchy was indicated by the fact that they were not apparent to the naked eye and that the Al 2p photopeak characteristic of Al^0 metal was clearly apparent in the spectra of all clean failed foil

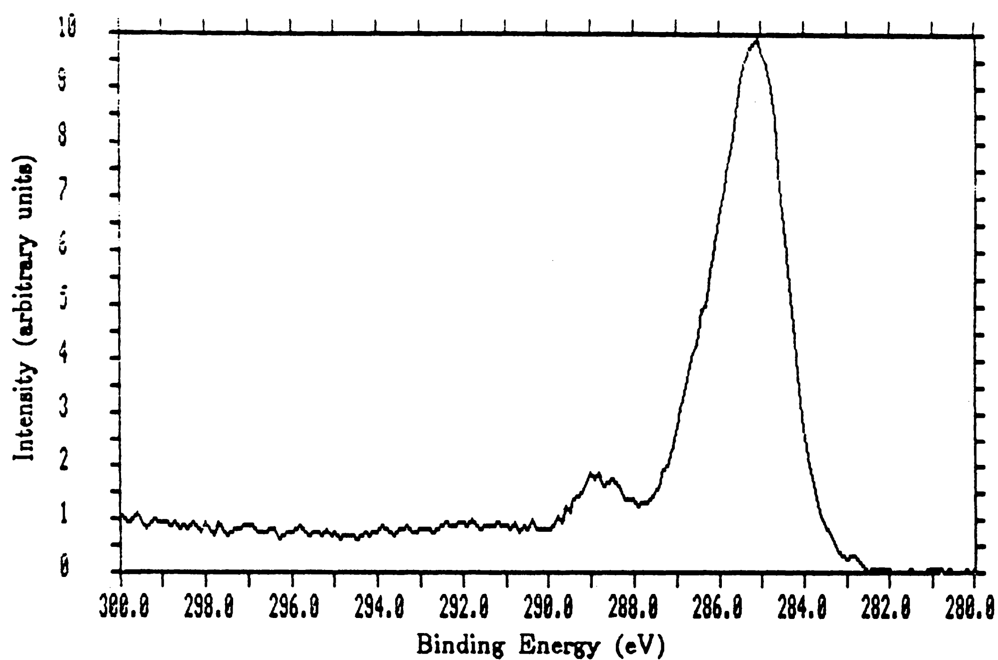

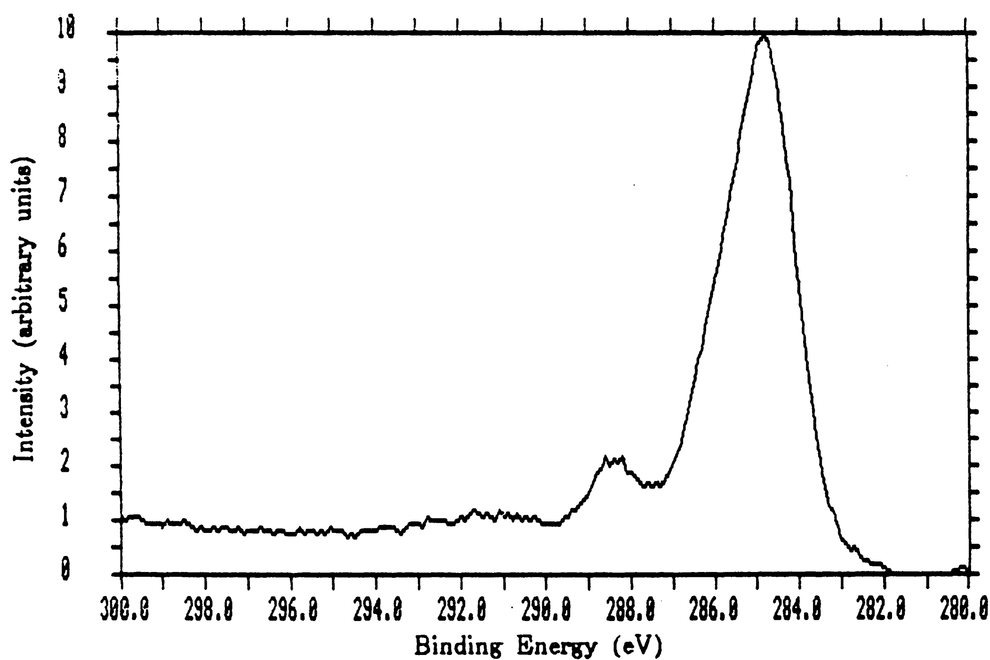

Figure 19. C 1s photopeaks obtained from (a) cured polyimide surface and (b) failed foil surface.

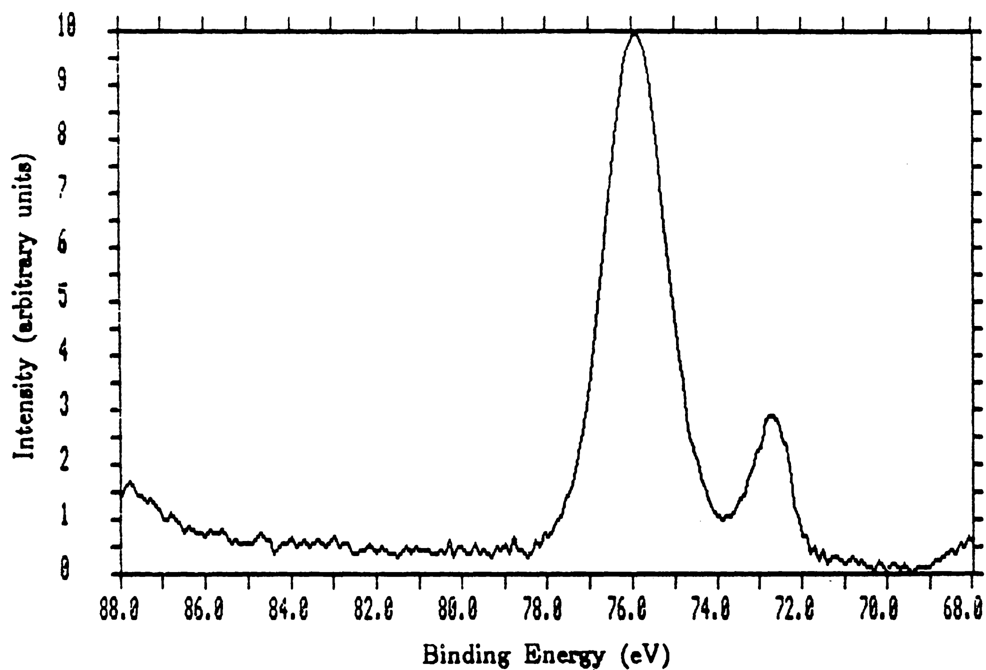

Figure 20. Al 2p photopeak obtained from failed foil surface, showing contribution from Al^0 as well as Al_2O_3.

surfaces. Figure 20 depicts such an Al photopeak. The main portion of the peak located at 75.9 eV is due to the native aluminum oxide of the foil surface. The smaller peak on the low binding energy side is attributed to elemental Al in the zero oxidation state. The fact that it appears at all indicates that a significant portion of the aluminum metal was covered by no more than 10 nm - the sampling depth of the XPS technique - of oxide, polymer or adventitious material. From the ratio of the heights of the two Al peaks - approximately 4:1 Al^{+3}:Al^0 - the oxide thickness was estimated at 3.8 nm. The expression used to calculate this value was reported by Wilson [93]:

$$d = \lambda \ln\left[\frac{\frac{D_b}{D_a} + \frac{I_b}{I_a}}{\frac{I_b}{I_a}} \right] \qquad \text{[IV.1]}$$

where d = the overlayer thickness, λ = mean free path of electrons in the two materials (assumed to be similar; here, $\lambda \simeq 2.1$ nm), D_a and D_b = atom densities of Al_2O_3 and Al^0 respectively, and I_a and I_b = peak intensities. The polyimide on the surface may have been present as a relatively continuous film less than approximately 6 nm thick, or as patches perhaps thicker but exposing the metal surface in other areas. As the sample area scanned by the XPS instrument is at least 10 mm square, the technique cannot resolve such surface distributions on a microscopic scale. The SEM image of a failed foil surface shown in Figure 18(a) suggests that polymer coverage was patchy. In contrast, judging from the SEM images in Figure 17(a), the undoped adhesive may leave a thin continuous film, or it may be patchy on a different scale than the doped material.

After the method of Lamb *et al.* [94], the relative proportions of C:N:O were calculated from the ideal molecular formula of BTDA/APB (see Figure 9) and compared to the same ratios calculated from XPS atomic concentrations on the specimen surfaces. The ratios for the ideal polyimide are C:N:O = 35:2:7. Table 5 lists atomic concentrations and XPS peak binding energies for an air-cured (through 300°C) undoped BTDA/APB surface and a cured $CoCl_2$ 1.0X-doped surface. Small amounts of SiO_2 were present on the doped polyimide surface, and the contribution to the oxygen signal from this oxide was corrected for in the listed C:N:O ratio. The presence of a small quantity of SiO_2 in this sample was thought to be due to the wearing of fitted glass surfaces of

containers used in the mixing of the polymer. Even after this correction, the proportion of oxygen on both surfaces was elevated in comparison to that of the ideal bulk polyimide. This elevation may have been due to an enrichment of oxygen-containing functional groups near the surfaces of the air-cured films. It is also possible that the oxygen concentration may have been elevated slightly by the presence of small amounts of residual BTDA/APB polyamic acid, for which the ideal C:N:O ratio is 35:2:8.

Representative XPS atomic concentrations and photopeak binding energies for adhesive surfaces and failed foil surfaces, both doped and undoped, are listed in Table 6. In general, the total and relative atomic percentages of carbon on the failed foil surfaces were less than those on the polyimide surfaces. Failed adhesive surfaces nearly always gave XPS atomic concentration ratios very similar to the ideal. Failed foil surfaces tended to be deficient in nitrogen and to have excess oxygen, nearly all of which could generally be considered to be associated with aluminum in the metal oxide.

The binding energy values of the N 1s, Cl 2p and Al 2p peaks remained constant within ± 0.1 eV, indicating that these elements were in similar oxidation states in the different surfaces. In the failed foil surfaces the O 1s peaks were shifted to lower binding energies in comparison to those on the failed adhesive surfaces and the cured polymer surfaces listed in Table 5. This shift of the O 1s peaks was due to the oxygen contribution from Al_2O_3. The Co 2p(3/2) peak from the failed adhesive side of the doped specimen was shifted to a higher binding energy relative to that of the failed foil side and that of the doped, air-cured surface listed in Table 5. The Co 2p(3/2) binding energy values from the latter two surfaces were similar to the 782.0 eV obtained from a sample of anhydrous $CoCl_2$ run in the spectrometer used for these experiments, but were a few eV less than the values reported by Frost *et al.* [95] for $CoCl_2$. The Co peak from the failed doped adhesive surface was relatively less intense than those from the other surfaces and was much more obscured by the nearby oxygen KVV Auger peaks. The overlapping O Auger signal contributed to the calculated Co concentration to make it similar to the concentration on the matching foil surface, though the actual Co signal on the adhesive side was less intense.

Table 5. Representative XPS atomic concentrations and binding energies for air-cured polyimide surfaces.

Surface	XPS Atomic Concentration (at %)						Binding Energy (eV) (C 1s = 285.0 eV)			
	C	N	O	Co	Cl	C:N:O	N 1s	O 1s	Co 2p	Cl 2p
BTDA/APB, undoped	70.1	4.0	21.4	–	–	35:2.0:10.6	400.5	532.5	–	–
BTDA/APB, $CoCl_2$ 1.0X	51.7	2.6	26.7	6.8	4.2	35:1.8:9.3	400.4	532.5	782.0	199.5

Table 6. Representative XPS atomic concentrations and binding energies for failed surfaces of peel specimens.

Failed Surface	XPS Atomic Concentration (at %) C	N	O	Co	Cl	Al	C:N:O*	Binding Energy (eV) (C 1s = 285.0 eV) N 1s	O 1s	Co 2p	Cl 2p	Al 2p
adhesive side, undoped	72.8	4.5	18.9	–	–	0.6	35:2.2:9.1	400.4	532.5	–	–	74.7
foil side, undoped	50.0	2.1	31.1	–	–	13.6	35:1.8:9.3	400.5	532.0	–	–	74.8†
adhesive side, $CoCl_2$ 1.0X	72.0	4.1	18.0	2.0	1.1	0.9	35:2.0:8.8	400.5	532.7	784.0	200.0	74.8
foil side, $CoCl_2$ 1.0X	50.2	2.6	29.4	1.9	1.0	13.5	35:1.8:6.4	400.6	532.0	782.5	199.1	74.8†

* Oxygen ratios corrected for oxide contributions

† B.E. values for Al_2O_3 peak; B.E. for Al° peak = 71.9 eV in both cases

The presence of dopant elements - Co and Cl - on the failed foil surfaces, even those of specimens in which the BTDA/APB layer originally cast on the foil was undoped, indicated that the dopant compound did in fact segregate toward the foil surface from the bulk of the polyimide. Figure 21 depicts representative Co 2p photopeaks obtained from failed adhesive and failed foil surfaces of specimens made with $CoCl_2$ 1.0X-doped adhesive. These spectra correspond to the same matched set of specimens for which the atomic concentrations were listed in Table 6. As stated previously, the Co signal from the failed adhesive surface was sufficiently weak to be partially obscured by the O Auger peaks. The satellite features of the peak from the failed foil surface are characteristic of Co(II) as oppposed to Co(III). In Co(III) photopeaks the height of the lower binding component in each pair of doublets is greatly increased with respect to the higher binding energy component. The added Co as $CoCl_2$ had therefore remained mostly as Co(II) in the adhesive bond, rather than converting largely to Co(III) as mixed oxides as reported by Rancourt *et al.*[42,43] and by Porta and Taylor [44]. A stoichiometric proportion of Co and Cl (1:2), however, was generally not observed, as can be seen from the data listed in Table 6; in many cases the surface Cl concentration as calculated from XPS data was significantly less than the Co concentration. On the other hand, the overall concentrations of these elements were usually just above the detection limit of the XPS instrument.

A relation called the *cobalt enrichment factor* (C.E.F.) was derived to express the relative concentration of Co on the failed foil surfaces. The proportion of Co to N on a surface as calculated from XPS spectra was related to the Co:N ratio as calculated from the nominal proportion of Co originally added to the polymer:

$$\text{C.E.F.} = \frac{\text{Co/N}_{(\text{from XPS analysis})}}{\text{Co/N}_{(\text{nominal concentration in polymer})}} \qquad \text{[IV.2]}$$

The Co concentration was referenced to that of N because measurable quantities of N were found only in the polymer surfaces, unlike C and O which were present in significant amounts on the metal surfaces as well. In addition, N concentration relative to those of the other elements fluctuated much less than, for example, the relative concentrations of C and O. C.E.F.s calculated from

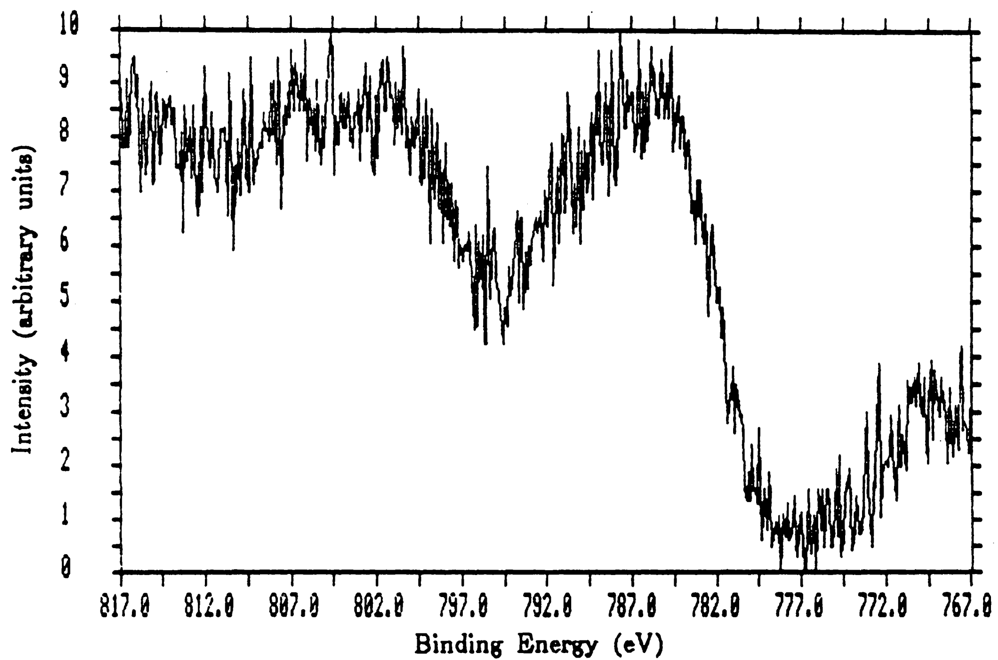

(a)

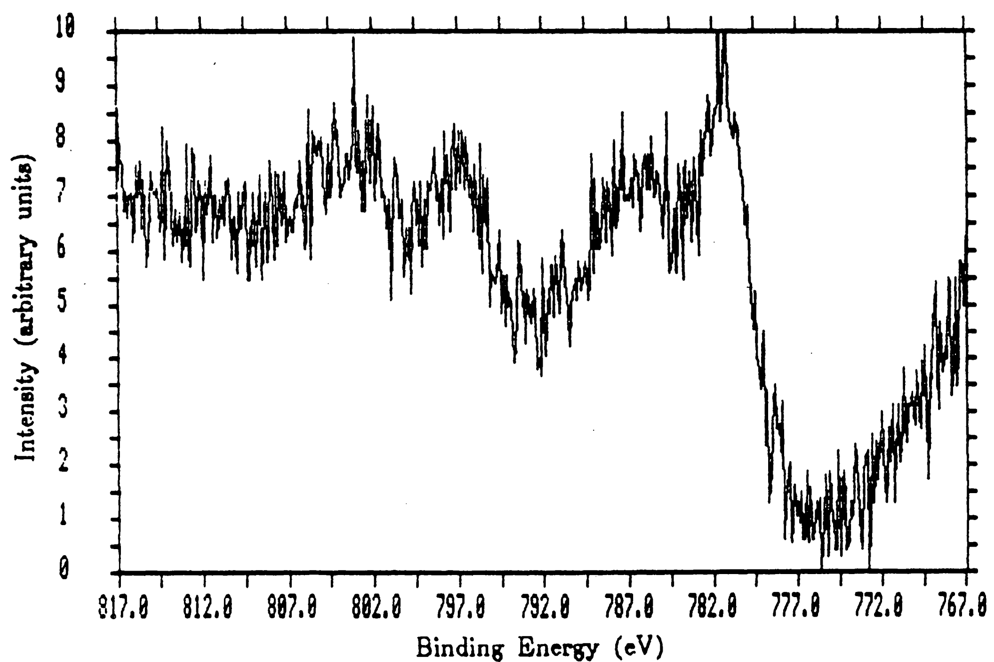

(b)

Figure 21. Co 2p photopeaks obtained from (a) failed adhesive surface and (b) failed foil surface.

the failed foil surfaces are listed in Table 7 along with peel strengths of the corresponding specimens. Owing to the relatively small values for total Co and N concentrations, calculated C.E.F.s can not be highly precise; the reported figures are rather meant to reflect trends.

Cobalt enrichment factors for 0.1X-doped specimens were consistently much higher than those from 1.0X-doped adhesive, although the total Co contents for the 0.1X surfaces were less. This is another indication that the dopant concentrated preferentially toward the metal surface. In general, the higher peel strengths occurred in the specimens having higher C.E.F.s. Cobalt enrichment factors for the matching adhesive surfaces were generally somewhat less than those of the foil surfaces, but in the same order of magnitude.

In light of the above observations, the following scheme for the bond structure and failure is suggested. The $CoCl_2$ dopant, assumed to have been homogeneously distributed in the polymer initially, preferentially concentrated near the adhesive-foil interface during the bonding process. Even if the undoped adhesive was originally cast on the foil, the dopant present migrated to the foil surface under these conditions of specimen preparation. It is assumed that dopant segregated toward the coupon surface as well, but that interface was not the one peeled apart in mechanical testing. Relatively large amounts of dopant, when present, concentrated to such a degree that the dopant material itself acted as a weak boundary layer along which failure occurred in peel. An illustration of this scheme is shown in Figure 22.

The actual shape and distribution of $CoCl_2$ deposits in this bonding situation at the nm level are not well characterized and the illustration is meant to be a schematic description only. In general layout this scheme is similar to the distributions of Co compounds in the films studied by Rancourt *et al.* [42,43]. Direct examination of the metal-adhesive interface *in situ* is difficult; the thickness and strength of the adherends make such techniques as microtoming or ion milling challenging. In an effort to characterize the dopant segregation, samples of free-standing adhesive layers were prepared by dissolving the foil adherends away from the polymer surface so that microtomed sections could be examined with TEM. However, as the water-soluble $CoCl_2$ did not convert to a less soluble compound, the dopant material was largely removed from the polymer by the aqueous NaOH solution used to dissolve the aluminum.

Table 7. Peel strengths and C.E.F.s for failed foil surfaces.

(a) Doped Film on Coupon

	0.1 X		1.0 X		Dopant Level
	200°C	300°C	200°C	300°C	Pre–cure Temperature
FPL etch	12.9	11.0	9.2	15.1	Peel Strength (N/cm)
	15.2	16.3	2.8	2.1	C.E.F.
NaOH etch	12.3	*	10.0	*	Peel Strength (N/cm)
	27.4		3.9		C.E.F.

(b) Doped Film on Foil

	0.1 X		1.0 X		Dopant Level
	200°C	300°C	200°C	300°C	Pre–cure Temperature
FPL etch	10.6	*	2.4	*	Peel Strength (N/cm)
	38.9		3.3		C.E.F.
NaOH etch	9.4	*	2.7	*	Peel Strength (N/cm)
	24.7		4.5		C.E.F.

* Specimen failed between the adhesive layers

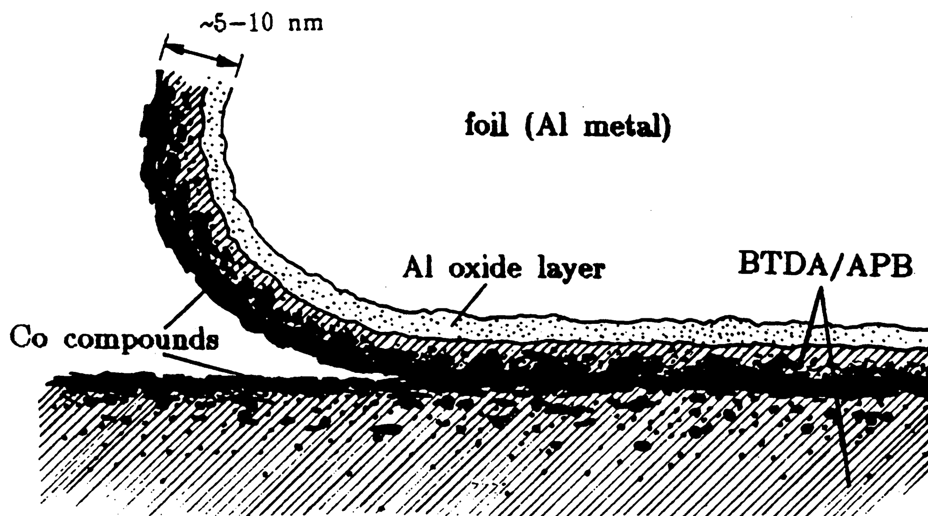

Figure 22. Suggested general scheme for bond structure and locus of failure.

C. Elevated Temperature Study

The results of a comparison of peel strengths of specimens tested at elevated temperature were inconclusive. A large proportion of both the doped and undoped specimens that could be tested failed between the adhesive layers; in addition, the foil adherends of many of the specimens tore while getting the peel strips started before placing them in the test fixture, and others tore during the course of testing. Thus, peel strengths for the adhesive-foil interface were not obtained in many cases. The problem of torn foil had been encountered before on infrequent occasions, but previously had not been responsible for the loss of so many specimens. Though no conclusive peel load vs. displacement traces were obtained, the failure surfaces of successfully tested specimens were visually examined and compared with their associated peel load plots. Small sections of some specimens did fail between the foil and the adhesive; the peel loads corresponding to these areas suggested that the $CoCl_2$ 1.0X-doped specimens did indeed maintain higher strengths beyond 190°C, the temperature at which the strength of undoped specimens began to fall off rapidly.

D. Environmental Exposure Study

The results of peel testing both doped and undoped specimens after hot water exposure are plotted as a function of exposure time in Figure 23. The peel strength of specimens made with neat BTDA/APB remained essentially unchanged after 100 hours of immersion in 70°C water. The strength of doped specimens dropped off linearly with exposure to about half the 1-hour value after 100 hours. Considering that the dopant compounds in the finished bonds were very likely still largely in the form of water-soluble $CoCl_2$, it is interesting that the doped specimens maintained peel strength to the extent that they did. Several of the doped specimens failed between the adhesive layers, and a film of water was evident between them when peeled apart. Otherwise, the failed

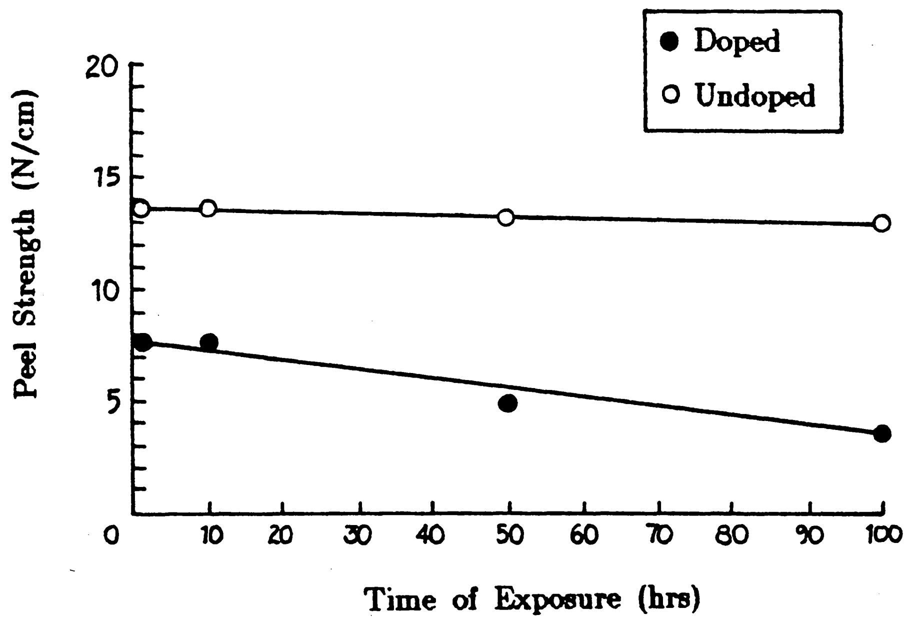

Figure 23. Effect of hot water (70°C) exposure prior to peel testing.

surfaces did not appear different from those of earlier tests. However, a sufficient number of specimens failed between the foil and adhesive to establish a clear trend of peel strength. As the neat polymer did not seem to be significantly affected by hot water exposure - given the ± 2.0 N/cm standard variation in peel strengths - the decrease in strength experienced by the doped specimens was due to the effect of water on the dopant or dopant-adhesive system. If liquid water was able to penetrate the bond to such an extent as to dissolve and leach out the doped material, then voids would remain behind in the adhesive and weaken the bond. However, no discoloration of the bath water indicating dissolved Co was noted during the experiment. Alternatively, any $CoCl_2$ remaining dissolved in the adhesive could interact with water so as to plasticize and weaken the polymer itself, which ordinarily would not be affected by water in the absence of the dopant.

Considering that widely variant results were obtained in earlier studies of metal modification of polyimides [8,9,39] for different polyimide/dopant systems, it is likely that the system chosen for this study is not necessarily optimal for the purpose of forming a graded, composite interface with an aluminum surface. It has been shown that an added metal salt in a polyimide can segregate toward a metal surface; a comprehensive study comparing many polymer/dopant combinations with respect to adhesive bonding and the characterization of interphase structures could very likely lead to the development of a microcomposite adhesive with improved bond properties.

V. Summary

A. Conclusions

The effects of $CoCl_2$ addition on the performance of a polyimide adhesive were investigated under a number of conditions, including the variation of curing parameters, elevated temperature testing, and environmental exposure. Results of peel testing and surface analysis in this regard led to the following conclusions:

- $CoCl_2$ added to BTDA/APB segregates in the adhesive during curing towards an aluminum surface.
- The segregation of $CoCl_2$ dopant toward an Al foil adherend has not been demonstrated to improve adhesion when tested in peel at room temperature.
- A $CoCl_2$ concentration of 1.0X resulted in lower peel strengths than 0.1X; both doping levels gave lower peel strengths than undoped BTDA/APB.

- FPL etch pretreatment results in significantly stronger bonds than simple degreasing, and slightly stronger bonds than NaOH etch.

- Since the undoped polyimide is more plastic than the doped material, it allows for fracture energy dissipation and resulted in higher peel strengths.

- The neat polyimide was unaffected by hot water exposure, while the doped system showed a linear decrease in peel strength with time.

B. Recommendations for Further Study

- Other polymer/dopant systems should be investigated; for example, the polymers studied by Taylor *et al.* [8-11,30,39-41], Rancourt *et al.* [42,43], and Bott [34]. It is possible that other dopants and/or polymer systems, similarly applied, may form graded near-surface regions more conducive to improved peel strength; e.g. a dopant distribution more similar to that shown in Figure 1 rather than the Co-rich layers formed in this study.

- Experiments should be conducted to determine whether the peel test specimen preparation procedure can be further refined. Though most of the specimens tested in this study were relatively strong in peel, it is possible that even better bonding would reveal more subtle variation in peel strength under different conditions. Procedural parameters to be experimented with include bonding temperature and pressure, cycle times spent under pressure, and bondline thickness.

- Different mechanical adhesion test methods should be used, such as the lap shear test, to compare the performance of adhesives in different loading situations; in addition, lap shear or

double cantilever beam specimens could be subjected to cyclic loading to evaluate the fatigue durability of bonds.

- Effects of environmental conditions, such as moisture or temperature cycling, should be further investigated. This and the preceding recommendation pertain to the to the evaluation of these doped polymers in terms of practical application in engineering designs.

- Study of the complexing of dopant metal ions in the polymer solution and the decomposition of metal compounds, similar to the work by Lyons *et al.* [96,97], is suggested.

VI. References

1. K. W. Allen, *Chemistry in Britain* **22**, 451 (1986).

2. G. P. Anderson, "Adhesion and Adhesives," *Encyclopedia of Physical Science and Technology* vol. 1 (Academic Press, Orlando, 1987).

3. P. M. Hergenrother, *Chemtech* **14**, 496 (1984).

4. ASM Committee on Failure Analysis of Weldments, "Failures of Weldments," *Failure Analysis and Prevention*, Metals Handbook 8th ed., vol. 10 (American Society for Metals, Metals Park, Ohio, 1975).

5. W. L. Jensen, "Failures of Mechanical Fasteners," *Failure Analysis and Prevention*, Metals Handbook 8th ed., vol. 10 (American Society for Metals, Metals Park, Ohio, 1975).

6. J. Schultz, L. Lavielle, and C. Martin, *J. Adhesion* **23**, 45 (1987).

7. C. U. Ko and J. P. Wightman, *J. Adhesion* **24**, 93 (1987).

8. L. T. Taylor and A. K. St. Clair, in *Polyimides* vol. 2, K. L. Mittal, Ed. (Plenum, New York, 1984).

9. L. T. Taylor, A. K. St. Clair, and NASA Langley Research Center, "Aluminum Ion Containing Adhesives," U. S. Patent No. 284,461 (1981).

10. T. L. Wohlford, J. Schaaf, L. T. Taylor, T. A. Furtsch, E. Khor, and A. K. St. Clair, in *Conductive Polymers*, R. B. Seymour, Ed. (Plenum, New York, 1981).

11. L. T. Taylor and A. K. St. Clair, *J. Appl. Polym. Sci.* **28**, 2393 (1983).

12. S. Mall, *J. Adhesion* **20**, 251 (1987).

13. H. F. Webster II, "Characterization of Thin Silicone Films Formed by Migration Across Defined Polymer Substrates," Master's thesis, Virginia Polytechnic Institute and State University (1986).

14. F. M. Fowkes, in *Chemistry and Physics of Interfaces* (American Chemical Society, Wash., DC, 1965).

15. A. W. Adamson, *Physical Chemistry of Surfaces* 4th ed. (John Wiley and Sons, New York, 1982).

16. D. J. Shaw, *Introduction to Colloid and Surface Chemistry* 3rd ed. (Butterworths, London, 1980).

17. B. O. Bateup, *Int. J. Adhesion and Adhesives* **1**, 233 (1981).

18. J. R. Huntsberger, *J. Adh.* **12**, 3 (1981).

19. A. J. Kinloch, "Adhesion: Fundamental Principles," *Encyclopedia of Materials Science and Engineering* vol. 1 (MIT Press, Cambridge, MA, 1986).

20. A. N. Gent and G. R. Hamed, "Adhesion and Bonding," *Encyclopedia of Polymer Science and Engineering* 2nd ed., vol. 1 (John Wiley and Sons, New York, 1988).

21. W. M. Edwards and E. I. DuPont DeNemours and Co., U.S. Patent Nos. 3,17:,614 and 3,179,634 (1965).

22. A. L. Endrey and E. I. DuPont DeNemours and Co., U.S. Patent Nos. 3,179,631 and 3,179,633 (1965).

23. L. W. Frost and I. Kesse, *J. Appl. Polym. Sci.* **8**, 1039 (1964).

24. H. A. Burgman *et al.*, *J. Appl. Polym. Sci.* **12**, 805 (1968).

25. D. J. Progar and T. L. St.Clair, *7th National SAMPE Tech. Conf. Ser.* **7**, 53 (1975).

26. J. W. Verbicky, Jr., "Polyimides," *Encyclopedia Polym. Sci. Engr.* 2nd ed., vol. 12 (John Wiley and Sons, New York, 1988).

27. M. L. Wallach, *J. Polym. Sci. Part A-2* **6**, 953 (1968).

28. J. D. Minford in *Durability of Structural Adhesives*, A. J. Kinloch, Ed. (Applied Science Publishers, London, 1983).

29. C. E. Carraher and M. Tsuda, eds., *Am. Chem. Soc. Symp. Ser.* **121** (American Chemical Society, Wash., DC, 1980).

30. A. K. St.Clair and L. T. Taylor, *J. Macromol. Sci.-Chem.* **A16**, 95 (1981).

31. E. P. Otocka, *J. Macromol. Sci. - Revs. Macromol. Chem.* **C5**, 275 (1971).

32. E. Bayer and V. Schurig, *Chemtech.* **6**, 212 (1976).

33. J. C. Anderson, U.S. Patent No. 4,109,052 (1978).

34. R. H. Bott, "Characterization of Modified Polyimide Adhesives," Ph.D. dissertation, Virginia Polytechnic Institute and State University (1988).

35. R. H. Angelo and E. I. DuPont DeNemours and Co., U.S. Patent No. 3,073,785 (1959).

36. N. S. Lidorenko, L. G. Gindin, B. N. Egorov, V. L. Kondratenkov, I. Y. Ravich and T. N. Toroptseva, *Doklady Akad. Nauk SSSR [Chem]* **187**, 581 (1969).

37. A. L. Endrey and E. I. DuPont DeNemours and Co., U.S. Patent No. 3,073,784 (1963).

38. M. N. Sarboluki, NASA Technical Brief, 3(2), item 36 (1978).

39. L. T. Taylor, V. C. Carver, T. A. Furtsch and A. K. St.Clair, *ACS Symp. Ser.* **121**, 71 (1980).

40. E. Khor and L. T. Taylor, *Macromolecules* **15**, 379 (1982).

41. S. A. Ezzell, T. A. Furtsch, E. Khor and L. T. Taylor, *J. Polym. Sci. Polym. Chem. Ed.* **21**, 865 (1983).

42. J. D. Rancourt and L. T. Taylor, *Macromolecules* **20**, 790 (1987).

43. J. D. Rancourt, R. K. Boggess, L. S. Horning and L. T. Taylor, *J. Electrochem. Soc.: Electrochem. Sci. Technol.* **134**, 85 (1987).

44. G. M. Porta and L. T. Taylor, *J. Mater. Res.* **3**, 211 (1988).

45. W. E. Haupin, "Aluminum," *Encyclopedia of Physical Science and Technology* vol. 1 (Academic Press, Orlando, FL, 1987).

46. W. A. Anderson and W. E. Haupin, "Aluminum and Aluminum Alloys," *Encyclopedia of Chemical Technology* 3rd ed., vol. 2 (John Wiley and Sons, New York, 1978).

47. N. N. Greenwood and A. Earnshaw, *Chemistry of the Elements* (Pergamon Press, Oxford, 1984) p. 243.

48. K. Wefers and C. Misra, "Oxides and Hydroxides of Aluminum," Alcoa Technical Paper No. 19, revised (Alcoa Laboratories, 1987).

49. J. P. Lyle and D. A. Granger, "Aluminum Alloys," *Ullmann's Encyclopedia of Industrial Chemistry* vol. 1 (VCH Publishers, Deerfield Beach, FL, 1985).

50. H. W. Eichner and W. E. Schowalter, Forest Products Laboratory Report No. 1813 (Madison, WI, 1950).

51. J. D. Venables, D. K. McNamara, J. M. Chen, T. S. Sun and R. L. Hopping, *Appl. Surf. Sci.* **3**, 88 (1979).

52. D. J. Packham, in *Adhesion Aspects of Polymeric Coatings* K. L. Mittal, Ed. (Plenum, New York, 1983).

53. D. J. Arrowsmith and A. W. Clifford, *Int. J. Adhesion and Adhesives* **3**, 193 (1983).

54. J. W. Diggle, T. C. Downie and C. W. Goulding, *Chem. Rev.* **69**, 365 (1969).

55. J. P. O'Sullivan and G. C. Wood, *Proc. Roy. Soc. Lond. A* **317**, 511 (1970).

56. S. Tajima, in *Advances in Corrosion Science and Technology* vol. 1 (Plenum, New York, 1970).

57. J. D. Venables, *J. Mater. Sci.* **19**, 2431 (1984).

58. G. D. Davis, J. S. Ahearn, L. J. Matienzo and J. D. Venables, *J. Mater. Sci.* **20**, 975 (1985).

59. D. A. Hardwick, J. S. Ahearn, A. Desai and J. D. Venables, *J. Mater. Sci.* **21**, 179 (1986).

60. L.-H. Lee, in *Adhesives, Sealants and Coatings for Space and Harsh Environments* (Plenum, New York, 1988).

61. R. A. Gledhill and A. J. Kinloch, *J. Adh.* **6**, 315 (1974).

62. J. Comyn, in *Durability of Structural Adhesives*, A. J. Kinloch, Ed. (Applied Science Publishers, London, 1983).

63. D. M. Brewis, in *ibid.*

64. A. J. Kinloch, in *Polymer Surfaces and Interfaces*, W. J. Feast and H. S. Munro, Eds. (John Wiley and Sons, Chichester, 1987).

65. J. D. Minford, in *High Performance Adhesive Bonding* 1st ed., Garry DeFrayne, Ed. (Society of Manufacturing Engineers, Dearborn, MI, 1983).

66. N. R. Farrar and K. H. G. Ashbee, *J. Phys. D: Appl. Phys.* **11**, 1009 (1978).

67. J. Nicholas and K. H. G. Ashbee, *J. Phys. D: Appl. Phys.* **11**, 1015 (1978).

68. D. J. Zalucha, in *High Performance Adhesive Bonding* 1st ed. Garry DeFrayne, Ed. (Society of Manufacturing Engineers, Dearborn, MI, 1983).

69. G. P. Anderson, S. J. Bennett and K. L. DeVries, *Analysis and Testing of Adhesive Bonds* (Academic Press, New York, 1977).

70. A. W. Bethune, *SAMPE J.* **11**, 4 (1975).

71. P. A. Koening, "Investigation of Acid/Base Interactions in Adhesion," Ph.D. dissertation, Virginia Polytechnic Institute and State University (1987).

72. A. N. Gent and G. R. Hamed, *Polym. Engr. Sci.* **17**, 462 (1977).

73. D. H. Kaeble, *Trans. Soc. Rheol.* **III**, 161 (1959).

74. D. H. Kaeble, *Trans. Soc. Rheol.* **IV**, 45 (1960).

75. J. J. Bikerman, *The Science of Adhesive Joints* (Academic Press, Orlando, FL, 1961).

76. R. D. Kemp, R. A. Brockman and G. J. Stenger, "A Study of the Floating Roller Peel Test for Adhesives," Interim Technical Report AFWAL-TR-87-4082 (Air Force Wright Aeronautical Laboratories Materials Laboratory, Wright-Patterson AFB, OH, 1987).

77. J. I. Goldstein, D. E. Newbury, P. Echlin, D. C. Joy, C. Fior and E. Lifshin, *Scanning Electron Microscopy and X-ray Microanalysis* (Plenum, New York, 1981).

78. A. Miller, Boeing Aircraft Co., personal communication.

79. K. Siegbahn, C. Nordling, A. Fahlman, R. Nordberg, K. Hamrin, J. Hedman, G. Johansson, T. Bergmark, S.-E. Karlsson, I. Lindgren and B. Lindberg, *ESCA - Atomic,*

Molecular and Solid State Structure Studied by Means of Electron Spectroscopy (North-Holland, Amsterdam, 1967).

80. J. F. Watts, *Surf. Interface Anal.* **12**, 497 (1988).

81. J. B. Hollenhead, "A Calorimetric Study of the Immersion of Bituminous Coal in Liquids," Master's thesis, Virginia Polytechnic Institute and State University (1988).

82. P. K. Ghosh, *Introduction to Photoelectron Spectroscopy* (John Wiley and Sons, New York, 1983).

83. T. A. Carlson, *Photoelectron and Auger Spectroscopy* (Plenum, New York, 1975).

84. C. J. Powell, in *Quantitative Surface Analysis of Materials*, N. S. McIntyre, Ed. ASTM Special Technical Publication 643 (ASTM, Philadelphia, 1978).

85. P. Swift, *Surf. Interface Anal.* **4**, 47 (1982).

86. S. Kohiki, *J. Elect. Spec. Rel. Phen.* **33**, 375 (1984).

87. S. Kohiki, *Appl. Surf. Sci.* **17** 497 (1984).

88. M. M. DiNardo, "Basic and Applied X-ray Photoelectron Spectroscopy of Complex Materials," Master's thesis, Virginia Polytechnic Institute and State University (1984).

89. R. E. Honig, *Thin Solid Films* **31**, 89 (1976).

90. K. Wefers and F. A. Mozelewski, *Aluminum* March (1988).

91. L. T. Taylor, personal communication.

92. A. N. Gent and R. P. Petrich, *Proc. Roy. Soc. A* **310**, 433 (1969).

93. G. R. Wilson, "Surface Studies of Aluminium and Aluminium Alloys," Ph.D. dissertation, University of Newcastle upon Tyne (1987).

94. R. N. Lamb, J. Baxter, M. Grunze, C. W. Kong and W. N. Unertl, *Langmuir* **4**, 249 (1988).

95. D. C. Frost, C. A. McDowell and I. S. Woolsey, *Molecular Physics* **27**, 1473 (1974).

96. A. M. Lyons, E. M. Pearce, M. J. Vasile, A. M. Mujsce and J. V. Waszczak, *ACS Symp. Ser.* **360**, 430 (1988).

97. A. M. Lyons, M. J. Vasile, E. M. Pearce and J. V. Waszczak, *Macromolecules* **21**, 3125 (1988).

The vita has been removed from the scanned document